

# Recursive Graphical Construction of Feynman Diagrams and Their Multiplicities in $\phi^4$ - and in $\phi^2 A$ -Theory

Hagen Kleinert<sup>1</sup>, Axel Pelster<sup>1</sup>, Boris Kastening<sup>2</sup>, and M. Bachmann<sup>1</sup>

<sup>1</sup>*Institut für Theoretische Physik, Freie Universität Berlin, Arnimallee 14, 14195 Berlin, Germany*

<sup>2</sup>*Institut für Theoretische Physik, Universität Heidelberg, Philosophenweg 16, 69120 Heidelberg, Germany*

The free energy of a field theory can be considered as a functional of the free correlation function. As such it obeys a nonlinear functional differential equation which can be turned into a recursion relation. This is solved order by order in the coupling constant to find all connected vacuum diagrams with their proper multiplicities. The procedure is applied to a multicomponent scalar field theory with a  $\phi^4$ -self-interaction and then to a theory of two scalar fields  $\phi$  and  $A$  with an interaction  $\phi^2 A$ . All Feynman diagrams with external lines are obtained from functional derivatives of the connected vacuum diagrams with respect to the free correlation function. Finally, the recursive graphical construction is automatized by computer algebra with the help of a unique matrix notation for the Feynman diagrams.

## I. INTRODUCTION

If one wants to draw all Feynman diagrams of higher orders by hand, it becomes increasingly difficult to identify all topologically different connections between the vertices. To count the corresponding multiplicities is an even more tedious task. Fortunately, there exist now various convenient computer programs, for instance *FeynArts* [1–3] or *QGraf* [4,5], for constructing and counting Feynman graphs in different field theories. These programs are based on a combinatorial enumeration of all possible ways of connecting vertices by lines according to Feynman’s rules.

The purpose of this paper is to develop an alternative systematic approach to construct all Feynman diagrams of a field theory. It relies on considering a Feynman diagram as a functional of its graphical elements, i.e. its lines and vertices. Functional derivatives with respect these elements are represented by graphical operations which remove lines or vertices of a Feynman diagram in all possible ways. With these operations, our approach proceeds in two steps. First the connected vacuum diagrams are constructed, together with their proper multiplicities, as solutions of a graphical recursion relation derived from a nonlinear functional differential equation. These relations have been set up a long time ago [6,7], but so far they have only been solved to all orders in the coupling strength in the trivial case of zero-dimensional quantum field theories. The present paper extends the previous work by developing an efficient graphical algorithm for solving this equation for two simple scalar field theories, a multicomponent scalar field theory with  $\phi^4$ -self-interaction and a theory with two scalar fields  $\phi$  and  $A$  with the interaction  $\phi^2 A$ . In a second step, all connected diagrams with external lines are obtained from functional derivatives of the connected vacuum diagrams with respect to the free correlation function. Finally, we automatize our construction method by computer algebra with the help of a unique matrix notation for Feynman diagrams.

## II. SCALAR $\phi^4$ -THEORY

Consider a self-interacting scalar field  $\phi$  with  $N$  components in  $d$  euclidean dimensions whose thermal fluctuations are controlled by the energy functional

$$E[\phi] = \frac{1}{2} \int_{12} G_{12}^{-1} \phi_1 \phi_2 + \frac{g}{4!} \int_{1234} V_{1234} \phi_1 \phi_2 \phi_3 \phi_4 \quad (2.1)$$

with some coupling constant  $g$ . In this short-hand notation, the spatial and tensorial arguments of the field  $\phi$ , the bilocal kernel  $G^{-1}$ , and the quartic interaction  $V$  are indicated by simple number indices, i.e.,

$$1 \equiv \{x_1, \alpha_1\}, \quad \int_1 \equiv \sum_{\alpha_1} \int d^d x_1, \quad \phi_1 \equiv \phi_{\alpha_1}(x_1), \quad G_{12}^{-1} \equiv G_{\alpha_1, \alpha_2}^{-1}(x_1, x_2), \quad V_{1234} \equiv V_{\alpha_1, \alpha_2, \alpha_3, \alpha_4}(x_1, x_2, x_3, x_4). \quad (2.2)$$

The kernel is a functional matrix  $G^{-1}$ , while  $V$  is a functional tensor, both being symmetric in their indices. The energy functional (2.1) describes generically  $d$ -dimensional euclidean  $\phi^4$ -theories. These are models for a family of universality classes of continuous phase transitions, such as the  $O(N)$ -symmetric  $\phi^4$ -theory which serves to derive

the critical phenomena in dilute polymer solutions ( $N = 0$ ), Ising- and Heisenberg-like magnets ( $N = 1, 3$ ), and superfluids ( $N = 2$ ). In all these cases, the energy functional (2.1) is specified by

$$G_{\alpha_1, \alpha_2}^{-1}(x_1, x_2) = \delta_{\alpha_1, \alpha_2} (-\partial_{x_1}^2 + m^2) \delta(x_1 - x_2), \quad (2.3)$$

$$V_{\alpha_1, \alpha_2, \alpha_3, \alpha_4}(x_1, x_2, x_3, x_4) = \frac{1}{3} \{ \delta_{\alpha_1, \alpha_2} \delta_{\alpha_3, \alpha_4} + \delta_{\alpha_1, \alpha_3} \delta_{\alpha_2, \alpha_4} + \delta_{\alpha_1, \alpha_4} \delta_{\alpha_2, \alpha_3} \} \delta(x_1 - x_2) \delta(x_1 - x_3) \delta(x_1 - x_4), \quad (2.4)$$

where the mass  $m^2$  is proportional to the temperature distance from the critical point. In the following we shall leave  $G^{-1}$  and  $V$  completely general, except for the symmetry with respect to their indices, and insert the physical values (2.3) and (2.4) at the end. By using natural units in which the Boltzmann constant  $k_B$  times the temperature  $T$  equals unity, the partition function is determined as a functional integral over the Boltzmann weight  $e^{-E[\phi]}$

$$Z = \int \mathcal{D}\phi e^{-E[\phi]} \quad (2.5)$$

and may be evaluated perturbatively as a power series in the coupling constant  $g$ . From this we obtain the negative free energy  $W = \ln Z$  as an expansion

$$W = \sum_{p=0}^{\infty} \frac{1}{p!} \left( \frac{-g}{4!} \right)^p W^{(p)}. \quad (2.6)$$

The coefficients  $W^{(p)}$  may be displayed as connected vacuum diagrams constructed from lines and vertices. Each line represents a free correlation function

$$1 \text{ --- } 2 \equiv G_{12}, \quad (2.7)$$

which is the functional inverse of the kernel  $G^{-1}$  in the energy functional (2.1), defined by

$$\int_2 G_{12} G_{23}^{-1} = \delta_{13}. \quad (2.8)$$

The vertices represent an integral over the interaction

$$\times \equiv \int_{1234} V_{1234}. \quad (2.9)$$

To construct all connected vacuum diagrams contributing to  $W^{(p)}$  to each order  $p$  in perturbation theory, one connects  $p$  vertices with  $4p$  legs in all possible ways according to Feynman's rules which follow from Wick's expansion of correlation functions into a sum of all pair contractions. This yields an increasing number of Feynman diagrams, each with a certain multiplicity which follows from combinatorics. In total there are  $4!^p p!$  ways of ordering the  $4p$  legs of the  $p$  vertices. This number is reduced by permutations of the legs and the vertices which leave a vacuum diagram invariant. Denoting the number of self-, double, triple and fourfold connections with  $S, D, T, F$ , there are  $2!^S, 2!^D, 3!^T, 4!^F$  leg permutations. An additional reduction arises from the number  $N$  of identical vertex permutations where the vertices remain attached to the lines emerging from them in the same way as before. The resulting multiplicity of a connected vacuum diagram in the  $\phi^4$ -theory is therefore given by the formula [8,9]

$$M_{\phi^4}^{E=0} = \frac{4!^p p!}{2!^{S+D} 3!^T 4!^F N}. \quad (2.10)$$

The superscript  $E$  records that the number of external legs of the connected vacuum diagrams is zero. The diagrammatic representation of the coefficients  $W^{(p)}$  in the expansion (2.6) of the negative free energy  $W$  is displayed in Table I up to five loops [10–12].

For higher orders, the factorially increasing number of diagrams makes it more and more difficult to construct all topologically different diagrams and to count their multiplicities. In particular, it becomes quite hard to identify by inspection the number  $N$  of identical vertex permutations. This identification problem is solved by introducing a unique matrix notation for the graphs, to be explained in detail in Section IV.

In the following, we shall generate iteratively all connected vacuum diagrams. We start in Subsection II.A by identifying graphical operations associated with functional derivatives with respect to the kernel  $G^{-1}$ , or the propagator  $G$ . In Subsection II.B we show that these operations can be applied to the one-loop contribution of the free partition function to generate all perturbative contributions to the partition function (2.5). In Subsection II.C we derive a nonlinear functional differential equation for the negative free energy  $W$ , whose graphical solution in Subsection II.D. yields all connected vacuum diagrams order by order in the coupling strength.

## A. Basic Graphical Operations

Each Feynman diagram is composed of integrals over products of free correlation functions  $G$  and may thus be considered as a functional of the kernel  $G^{-1}$ . The connected vacuum diagrams satisfy a certain functional differential equation, from which they will be constructed recursively. This will be done by a graphical procedure, for which we set up the necessary graphical rules in this subsection. First we observe that functional derivatives with respect to the kernel  $G^{-1}$  or to the free propagator  $G$  correspond to the graphical prescriptions of cutting or of removing a single line of a diagram in all possible ways, respectively.

### 1. Cutting Lines

Since  $\phi$  is a real scalar field, the kernel  $G^{-1}$  is a symmetric functional matrix. This property has to be taken into account when performing functional derivatives with respect to the kernel  $G^{-1}$ , whose basic rule is

$$\frac{\delta G_{12}^{-1}}{\delta G_{34}^{-1}} = \frac{1}{2} \{ \delta_{13} \delta_{42} + \delta_{14} \delta_{32} \}. \quad (2.11)$$

From the identity (2.8) and the functional chain rule, we find the effect of this derivative on the free propagator

$$-2 \frac{\delta G_{12}}{\delta G_{34}^{-1}} = G_{13} G_{42} + G_{14} G_{32}. \quad (2.12)$$

This has the graphical representation

$$-2 \frac{\delta}{\delta G_{34}^{-1}} \begin{array}{c} 1 \\ \text{---} \\ 2 \end{array} = \begin{array}{c} 1 \\ \text{---} \\ 3 \end{array} \begin{array}{c} 4 \\ \text{---} \\ 2 \end{array} + \begin{array}{c} 1 \\ \text{---} \\ 4 \end{array} \begin{array}{c} 3 \\ \text{---} \\ 2 \end{array}. \quad (2.13)$$

Thus differentiating a propagator with respect to the kernel  $G^{-1}$  amounts to cutting the associated line into two pieces. The differentiation rule (2.11) ensures that the spatial indices of the kernel are symmetrically attached to the newly created line ends in the two possible ways. When differentiating a general Feynman integral with respect to  $G^{-1}$ , the product rule of functional differentiation leads to a sum of diagrams in which each line is cut once.

With this graphical operation, the product of two fields can be rewritten as a derivative of the energy functional with respect to the kernel

$$\phi_1 \phi_2 = 2 \frac{\delta E[\phi]}{\delta G_{12}^{-1}}, \quad (2.14)$$

as follows directly from (2.1) and (2.11). Applying the substitution rule (2.14) to the functional integral for the fully interacting two-point function

$$\mathbf{G}_{12} = \frac{1}{Z} \int \mathcal{D}\phi \phi_1 \phi_2 e^{-E[\phi]}, \quad (2.15)$$

we obtain the fundamental identity

$$\mathbf{G}_{12} = -2 \frac{\delta W}{\delta G_{12}^{-1}}. \quad (2.16)$$

Thus, by cutting a line of the connected vacuum diagrams in all possible ways, we obtain all diagrams of the fully interacting two-point function. Analytically this has a Taylor series expansion in powers of the coupling constant  $g$  similar to (2.6)

$$\mathbf{G}_{12} = \sum_{p=0}^{\infty} \frac{1}{p!} \left( \frac{-g}{4!} \right)^p \mathbf{G}_{12}^{(p)} \quad (2.17)$$

with coefficients

$$\mathbf{G}_{12}^{(p)} = -2 \frac{\delta W^{(p)}}{\delta G_{12}^{-1}}. \quad (2.18)$$

The cutting prescription (2.16) converts the vacuum diagrams of  $p$ th order in the coefficients  $W^{(p)}$  in Table I to the corresponding ones in the coefficients  $\mathbf{G}_{12}^{(p)}$  of the two-point function. The results are shown in Table II up to four loops. The numbering of diagrams used in Table II reveals from which connected vacuum diagrams they are obtained by cutting a line. For instance, the diagrams #15.1-#15.5 and their multiplicities in Table II follow from the connected vacuum diagram #15 in Table I. We observe that the multiplicity of a diagram of a two-point function obeys a formula similar to (2.10):

$$M_{\phi^4}^{E=2} = \frac{4!^p p! 2!}{2!^{S+D} 3!^T N}. \quad (2.19)$$

In the numerator, the  $4!^p p!$  permutations of the  $4p$  legs of the  $p$  vertices are multiplied by a factor  $2!$  for the permutations of the  $E = 2$  end points of the two-point function. The number  $N$  in the denominator counts the identical permutations of both the  $p$  vertices and the two end points.

Performing a differentiation of the two-point function (2.15) with respect to the kernel  $G^{-1}$  yields

$$-2 \frac{\delta \mathbf{G}_{12}}{\delta G_{34}^{-1}} = \mathbf{G}_{1234} - \mathbf{G}_{12} \mathbf{G}_{34}, \quad (2.20)$$

where  $\mathbf{G}_{1234}$  denotes the fully interacting four-point function

$$\mathbf{G}_{1234} = \frac{1}{Z} \int \mathcal{D}\phi \phi_1 \phi_2 \phi_3 \phi_4 e^{-E[\phi]}. \quad (2.21)$$

The term  $\mathbf{G}_{12} \mathbf{G}_{34}$  in (2.20) subtracts a certain set of disconnected diagrams from  $\mathbf{G}_{1234}$ . By subtracting *all* disconnected diagrams from  $\mathbf{G}_{1234}$ , we obtain the connected four-point function

$$\mathbf{G}_{1234}^c \equiv \mathbf{G}_{1234} - \mathbf{G}_{12} \mathbf{G}_{34} - \mathbf{G}_{13} \mathbf{G}_{24} - \mathbf{G}_{14} \mathbf{G}_{23} \quad (2.22)$$

in the form

$$\mathbf{G}_{1234}^c = -2 \frac{\delta \mathbf{G}_{12}}{\delta G_{34}^{-1}} - \mathbf{G}_{13} \mathbf{G}_{24} - \mathbf{G}_{14} \mathbf{G}_{23}. \quad (2.23)$$

The first term contains all diagrams obtained by cutting a line in the diagrams of the two-point-function  $\mathbf{G}_{12}$ . The second and third terms remove from these the disconnected diagrams. In this way we obtain the perturbative expansion

$$\mathbf{G}_{1234}^c = \sum_{p=1}^{\infty} \frac{1}{p!} \left( \frac{-g}{4!} \right)^p \mathbf{G}_{1234}^{c,(p)} \quad (2.24)$$

with coefficients

$$\mathbf{G}_{1234}^{c,(p)} = -2 \frac{\delta \mathbf{G}_{12}^{(p)}}{\delta G_{34}^{-1}} - \sum_{q=0}^p \binom{p}{q} \left( \mathbf{G}_{13}^{(p-q)} \mathbf{G}_{24}^{(q)} + \mathbf{G}_{14}^{(p-q)} \mathbf{G}_{23}^{(q)} \right). \quad (2.25)$$

They are listed diagrammatically in Table III up to three loops. As before in Table II, the multiple numbering in Table III indicates the origin of each diagram of the connected four-point function. For instance, the diagram #11.2.2, #11.4.3, #14.1.2, #14.3.3 in Table III stems together with its multiplicity from the diagrams #11.2, #11.4, #14.1, #14.3 in Table II.

The multiplicity of each diagram of a connected four-point function obeys a formula similar to (2.19):

$$M_{\phi^4}^{E=4} = \frac{4!^p p! 4!}{2!^{S+D} 3!^T N}. \quad (2.26)$$

This multiplicity decomposes into equal parts if the spatial indices 1, 2, 3, 4 are assigned to the  $E = 4$  end points of the connected four-point function, for instance:

$$62208 \quad \begin{array}{c} \diagup \quad \diagdown \\ \circ \quad \circ \\ \diagdown \quad \diagup \end{array} \equiv 20736 \begin{array}{c} 1 \quad 3 \\ \diagdown \quad \diagup \\ \circ \quad \circ \\ \diagup \quad \diagdown \\ 2 \quad 4 \end{array} + 20736 \begin{array}{c} 1 \quad 2 \\ \diagdown \quad \diagup \\ \circ \quad \circ \\ \diagup \quad \diagdown \\ 3 \quad 4 \end{array} + 20736 \begin{array}{c} 1 \quad 2 \\ \diagdown \quad \diagup \\ \circ \quad \circ \\ \diagup \quad \diagdown \\ 4 \quad 3 \end{array} . \quad (2.27)$$

Generalizing the multiplicities (2.10), (2.19), and (2.26) for connected vacuum diagrams, two- and four-point functions to an arbitrary connected correlation function with an even number  $E$  of end points, we see that

$$M_{\phi^4}^E = \frac{4!^p p! E!}{2!^{S+D} 3!^T 4!^F N}, \quad (2.28)$$

where  $N$  counts the number of permutations of vertices and external lines which leave the diagram unchanged.

## 2. Removing Lines

We now study the graphical effect of functional derivatives with respect to the free propagator  $G$ , where the basic differentiation rule (2.11) becomes

$$\frac{\delta G_{12}}{\delta G_{34}} = \frac{1}{2} \{ \delta_{13} \delta_{42} + \delta_{14} \delta_{32} \}. \quad (2.29)$$

We represent this graphically by extending the elements of Feynman diagrams by an open dot with two labeled line ends representing the delta function:

$$1 \text{---} \circ \text{---} 2 = \delta_{12}. \quad (2.30)$$

Thus we can write the differentiation (2.29) graphically as follows:

$$\frac{\delta}{\delta 3 \text{---} 4} \quad 1 \text{---} 2 = \frac{1}{2} \left\{ 1 \text{---} \circ \text{---} 3 \quad 4 \text{---} \circ \text{---} 2 \quad + \quad 1 \text{---} \circ \text{---} 4 \quad 3 \text{---} \circ \text{---} 2 \right\}. \quad (2.31)$$

Differentiating a line with respect to the free correlation function removes the line, leaving in a symmetrized way the spatial indices of the free correlation function on the vertices to which the line was connected.

The effect of this derivative is illustrated by studying the diagrammatic effect of the operator

$$\hat{L} = \int_{12} G_{12} \frac{\delta}{\delta G_{12}}. \quad (2.32)$$

Applying  $\hat{L}$  to a connected vacuum diagram in  $W^{(p)}$ , the functional derivative  $\delta/\delta G_{12}$  removes successively each of its  $2p$  lines. Subsequently, the removed lines are again reinserted, so that the connected vacuum diagrams  $W^{(p)}$  are eigenfunctions of  $\hat{L}$ , whose eigenvalues  $2p$  count the lines of the diagrams:

$$\hat{L} W^{(p)} = 2p W^{(p)}. \quad (2.33)$$

As an example, take the explicit first-order expression for the vacuum diagrams, i.e.

$$W^{(1)} = 3 \int_{1234} V_{1234} G_{12} G_{34}, \quad (2.34)$$

and apply the basic rule (2.29), leading to the desired eigenvalue 2.

## B. Perturbation Theory

Field theoretic perturbation expressions are usually derived by introducing an external current  $J$  into the energy functional (2.1) which is linearly coupled to the field  $\phi$  [13–15]. Thus the partition function (2.5) becomes in the presence of  $J$  the generating functional  $Z[J]$  which allows us to find all free  $n$ -point functions from functional derivatives with respect to this external current  $J$ . In the normal phase of a  $\phi^4$ -theory, the expectation value of the field  $\phi$  is zero and only correlation functions of an even number of fields are nonzero. To calculate all of these, it is possible to substitute two functional derivatives with respect to the current  $J$  by one functional derivative with respect to the kernel  $G^{-1}$ . This reduces the number of functional derivatives in each order of perturbation theory by one half and has the additional advantage that the introduction of the current  $J$  becomes superfluous.

## 1. Current Approach

Recall briefly the standard perturbative treatment, in which the energy functional (2.1) is artificially extended by a source term

$$E[\phi, J] = E[\phi] - \int_1 J_1 \phi_1. \quad (2.35)$$

The functional integral for the generating functional

$$Z[J] = \int \mathcal{D}\phi e^{-E[\phi, J]} \quad (2.36)$$

is first explicitly calculated for a vanishing coupling constant  $g$ , yielding

$$Z^{(0)}[J] = \exp \left\{ -\frac{1}{2} \text{Tr} \ln G^{-1} + \frac{1}{2} \int_{12} G_{12} J_1 J_2 \right\}, \quad (2.37)$$

where the trace of the logarithm of the kernel is defined by the series [16, p. 16]

$$\text{Tr} \ln G^{-1} = \sum_{n=1}^{\infty} \frac{(-1)^{n+1}}{n} \int_{1\dots n} \{G_{12}^{-1} - \delta_{12}\} \cdots \{G_{n1}^{-1} - \delta_{n1}\}. \quad (2.38)$$

If the coupling constant  $g$  does not vanish, one expands the generating functional  $Z[J]$  in powers of the quartic interaction  $V$ , and reexpresses the resulting powers of the field within the functional integral (2.36) as functional derivatives with respect to the current  $J$ . The original partition function (2.5) can thus be obtained from the free generating functional (2.37) by the formula

$$Z = \exp \left\{ -\frac{g}{4!} \int_{1234} V_{1234} \frac{\delta^4}{\delta J_1 \delta J_2 \delta J_3 \delta J_4} \right\} Z^{(0)}[J] \Big|_{J=0}. \quad (2.39)$$

Expanding the exponential in a power series, we arrive at the perturbation expansion

$$Z = \left\{ 1 + \frac{-g}{4!} \int_{1234} V_{1234} \frac{\delta^4}{\delta J_1 \delta J_2 \delta J_3 \delta J_4} + \frac{1}{2} \left( \frac{-g}{4!} \right)^2 \int_{12345678} V_{1234} V_{5678} \frac{\delta^8}{\delta J_1 \delta J_2 \delta J_3 \delta J_4 \delta J_5 \delta J_6 \delta J_7 \delta J_8} + \dots \right\} Z^{(0)}[J] \Big|_{J=0}, \quad (2.40)$$

in which the  $p$ th order contribution for the partition function requires the evaluation of  $4p$  functional derivatives with respect to the current  $J$ .

## 2. Kernel Approach

The derivation of the perturbation expansion simplifies, if we use functional derivatives with respect to the kernel  $G^{-1}$  in the energy functional (2.1) rather than with respect to the current  $J$ . This allows us to substitute the previous expression (2.39) for the partition function by

$$Z = \exp \left\{ -\frac{g}{6} \int_{1234} V_{1234} \frac{\delta^2}{\delta G_{12}^{-1} \delta G_{34}^{-1}} \right\} e^{W^{(0)}}, \quad (2.41)$$

where the zeroth order of the negative free energy has the diagrammatic representation

$$W^{(0)} = -\frac{1}{2} \text{Tr} \ln G^{-1} \equiv \frac{1}{2} \bigcirc. \quad (2.42)$$

Expanding again the exponential in a power series, we obtain

$$Z = \left\{ 1 + \frac{-g}{6} \int_{1234} V_{1234} \frac{\delta^2}{\delta G_{12}^{-1} \delta G_{34}^{-1}} + \frac{1}{2} \left( \frac{-g}{6} \right)^2 \int_{12345678} V_{1234} V_{5678} \frac{\delta^4}{\delta G_{12}^{-1} \delta G_{34}^{-1} \delta G_{56}^{-1} \delta G_{78}^{-1}} + \dots \right\} e^{W^{(0)}}. \quad (2.43)$$

Thus we need only half as many functional derivatives than in (2.40). Taking into account (2.11), (2.12), and (2.38), we obtain

$$\frac{\delta W^{(0)}}{\delta G_{12}^{-1}} = -\frac{1}{2} G_{12}, \quad \frac{\delta^2 W^{(0)}}{\delta G_{12}^{-1} \delta G_{34}^{-1}} = \frac{1}{4} \{G_{13} G_{24} + G_{14} G_{23}\}, \quad (2.44)$$

such that the partition function  $Z$  becomes

$$Z = \left\{ 1 + \frac{-g}{4!} 3 \int_{1234} V_{1234} G_{12} G_{34} + \frac{1}{2} \left( \frac{-g}{4!} \right)^2 \int_{12345678} V_{1234} V_{5678} \right. \\ \left. \times \left[ 9 G_{12} G_{34} G_{56} G_{78} + 24 G_{15} G_{26} G_{37} G_{48} + 72 G_{12} G_{35} G_{46} G_{78} \right] + \dots \right\} e^{W^{(0)}}. \quad (2.45)$$

This has the diagrammatic representation

$$Z = \left\{ 1 + \frac{-g}{4!} 3 \text{ (two circles)} + \frac{1}{2} \left( \frac{-g}{4!} \right)^2 \left[ 9 \text{ (two circles)} \text{ (two circles)} + 24 \text{ (two circles with a line)} + 72 \text{ (two circles)} \right] + \dots \right\} e^{W^{(0)}}. \quad (2.46)$$

All diagrams in this expansion follow directly by successively cutting lines of the basic one-loop vacuum diagram (2.42) according to (2.43). By going to the logarithm of the partition function  $Z$ , we find a diagrammatic expansion for the negative free energy  $W$

$$W = \frac{1}{2} \text{ (circle)} + \frac{-g}{4!} 3 \text{ (two circles)} + \frac{1}{2} \left( \frac{-g}{4!} \right)^2 \left\{ 24 \text{ (two circles with a line)} + 72 \text{ (two circles)} \right\} + \dots, \quad (2.47)$$

which turns out to contain precisely all connected diagrams in (2.46) with the same multiplicities. In the next section we show that this diagrammatic expansion for the negative free energy can be derived more efficiently by solving a differential equation.

### C. Functional Differential Equation for $W = \ln Z$

Regarding the partition function  $Z$  as a functional of the kernel  $G^{-1}$ , we derive a functional differential equation for  $Z$ . We start with the trivial identity

$$\int \mathcal{D}\phi \frac{\delta}{\delta \phi_1} \left\{ \phi_2 e^{-E[\phi]} \right\} = 0, \quad (2.48)$$

which follows via functional integration by parts from the vanishing of the exponential at infinite fields. Taking into account the explicit form of the energy functional (2.1), we perform the functional derivative with respect to the field and obtain

$$\int \mathcal{D}\phi \left\{ \delta_{12} - \int_3 G_{13}^{-1} \phi_2 \phi_3 - \frac{g}{6} \int_{345} V_{1345} \phi_2 \phi_3 \phi_4 \phi_5 \right\} e^{-E[\phi]} = 0. \quad (2.49)$$

Applying the substitution rule (2.14), this equation can be expressed in terms of the partition function (2.5) and its derivatives with respect to the kernel  $G^{-1}$ :

$$\delta_{12} Z + 2 \int_3 G_{13}^{-1} \frac{\delta Z}{\delta G_{23}^{-1}} = \frac{2}{3} g \int_{345} V_{1345} \frac{\delta^2 Z}{\delta G_{23}^{-1} \delta G_{45}^{-1}}. \quad (2.50)$$

Note that this linear functional differential equation for the partition function  $Z$  is, indeed, solved by (2.41) due to the commutation relation

$$\exp \left\{ -\frac{g}{6} \int_{1234} V_{1234} \frac{\delta^2}{\delta G_{12}^{-1} \delta G_{34}^{-1}} \right\} G_{56}^{-1} - G_{56}^{-1} \exp \left\{ -\frac{g}{6} \int_{1234} V_{1234} \frac{\delta^2}{\delta G_{12}^{-1} \delta G_{34}^{-1}} \right\} \\ = -\frac{g}{3} \int_{78} V_{5678} \frac{\delta}{\delta G_{78}^{-1}} \exp \left\{ -\frac{g}{6} \int_{1234} V_{1234} \frac{\delta^2}{\delta G_{12}^{-1} \delta G_{34}^{-1}} \right\} \quad (2.51)$$

which follows from the canonical one

$$\frac{\delta}{\delta G_{12}^{-1}} G_{34}^{-1} - G_{34}^{-1} \frac{\delta}{\delta G_{12}^{-1}} = \frac{1}{2} \{ \delta_{13} \delta_{24} + \delta_{14} \delta_{23} \}. \quad (2.52)$$

Going over from  $Z$  to  $W = \ln Z$ , the linear functional differential equation (2.50) turns into a nonlinear one:

$$\delta_{12} + 2 \int_3 G_{13}^{-1} \frac{\delta W}{\delta G_{23}^{-1}} = \frac{2}{3} g \int_{345} V_{1345} \left\{ \frac{\delta^2 W}{\delta G_{23}^{-1} \delta G_{45}^{-1}} + \frac{\delta W}{\delta G_{23}^{-1}} \frac{\delta W}{\delta G_{45}^{-1}} \right\}. \quad (2.53)$$

If the coupling constant  $g$  vanishes, this is immediately solved by (2.42). For a non-vanishing coupling constant  $g$ , the right-hand side in (2.53) produces corrections to (2.42) which we shall denote with  $W^{(\text{int})}$ . Thus the negative free energy  $W$  decomposes according to

$$W = W^{(0)} + W^{(\text{int})}. \quad (2.54)$$

Inserting this into (2.53) and taking into account (2.44), we obtain the following functional differential equation for the interaction negative free energy  $W^{(\text{int})}$ :

$$\begin{aligned} \int_{12} G_{12}^{-1} \frac{\delta W^{(\text{int})}}{\delta G_{12}^{-1}} &= \frac{g}{4} \int_{1234} V_{1234} G_{12} G_{34} - \frac{g}{3} \int_{1234} V_{1234} G_{12} \frac{\delta W^{(\text{int})}}{\delta G_{34}^{-1}} \\ &+ \frac{g}{3} \int_{1234} V_{1234} \left\{ \frac{\delta^2 W^{(\text{int})}}{\delta G_{12}^{-1} \delta G_{34}^{-1}} + \frac{\delta W^{(\text{int})}}{\delta G_{12}^{-1}} \frac{\delta W^{(\text{int})}}{\delta G_{34}^{-1}} \right\}. \end{aligned} \quad (2.55)$$

With the help of the functional chain rule, the first and second derivatives with respect to the kernel  $G^{-1}$  are rewritten as

$$\frac{\delta}{\delta G_{12}^{-1}} = - \int_{34} G_{13} G_{24} \frac{\delta}{\delta G_{34}} \quad (2.56)$$

and

$$\begin{aligned} \frac{\delta^2}{\delta G_{12}^{-1} \delta G_{34}^{-1}} &= \int_{5678} G_{15} G_{26} G_{37} G_{48} \frac{\delta^2}{\delta G_{56} \delta G_{78}} \\ &+ \frac{1}{2} \int_{56} \{ G_{13} G_{25} G_{46} + G_{14} G_{25} G_{36} + G_{23} G_{15} G_{46} + G_{24} G_{15} G_{36} \} \frac{\delta}{\delta G_{56}}, \end{aligned} \quad (2.57)$$

respectively, so that the functional differential equation (2.55) for  $W^{(\text{int})}$  takes the form (compare Eq. (51) in Ref. [7])

$$\begin{aligned} \int_{12} G_{12} \frac{\delta W^{(\text{int})}}{\delta G_{12}} &= -\frac{g}{4} \int_{1234} V_{1234} G_{12} G_{34} - g \int_{123456} V_{1234} G_{12} G_{35} G_{46} \frac{\delta W^{(\text{int})}}{\delta G_{56}} \\ &- \frac{g}{3} \int_{12345678} V_{1234} G_{15} G_{26} G_{37} G_{48} \left\{ \frac{\delta^2 W^{(\text{int})}}{\delta G_{56} \delta G_{78}} + \frac{\delta W^{(\text{int})}}{\delta G_{56}} \frac{\delta W^{(\text{int})}}{\delta G_{78}} \right\}. \end{aligned} \quad (2.58)$$

#### D. Recursion Relation and Graphical Solution

We now convert the functional differential equation (2.58) into a recursion relation by expanding  $W^{(\text{int})}$  into a power series in  $G$ :

$$W^{(\text{int})} = \sum_{p=1}^{\infty} \frac{1}{p!} \left( \frac{-g}{4!} \right)^p W^{(p)}. \quad (2.59)$$

Using the property (2.33) that the coefficient  $W^{(p)}$  satisfies the eigenvalue problem of the line numbering operator (2.32), we obtain the recursion relation



$$\begin{aligned}
W^{(p+1)} &= 12 \int_{123456} V_{1234} G_{12} G_{35} G_{46} \frac{\delta W^{(p)}}{\delta G_{56}} + 4 \int_{12345678} V_{1234} G_{15} G_{26} G_{37} G_{48} \frac{\delta^2 W^{(p)}}{\delta G_{56} \delta G_{78}} \\
&\quad + 4 \sum_{q=1}^{p-1} \binom{p}{q} \int_{12345678} V_{1234} G_{15} G_{26} G_{37} G_{48} \frac{\delta W^{(p-q)}}{\delta G_{56}} \frac{\delta W^{(q)}}{\delta G_{78}}
\end{aligned} \tag{2.60}$$

and the initial condition (2.34). With the help of the graphical rules of Subsection II A, the recursion relation (2.60) can be written diagrammatically as follows

$$\begin{aligned}
W^{(p+1)} &= 4 \frac{\delta^2 W^{(p)}}{\delta 1 \text{---} 2 \delta 3 \text{---} 4} \begin{array}{c} 1 \\ 2 \\ 3 \\ 4 \end{array} \begin{array}{c} \diagup \\ \diagdown \\ \diagup \\ \diagdown \end{array} + 12 \frac{\delta W^{(p)}}{\delta 1 \text{---} 2} \begin{array}{c} 1 \\ 2 \end{array} \begin{array}{c} \diagup \\ \diagdown \end{array} \\
&\quad + 4 \sum_{q=1}^{p-1} \binom{p}{q} \frac{\delta W^{(p-q)}}{\delta 1 \text{---} 2} \begin{array}{c} 1 \\ 2 \end{array} \begin{array}{c} \diagup \\ \diagdown \end{array} \begin{array}{c} 3 \\ 4 \end{array} \frac{\delta W^{(q)}}{\delta 3 \text{---} 4}, \quad p \geq 1.
\end{aligned} \tag{2.61}$$

This is iterated starting from

$$W^{(1)} = 3 \begin{array}{c} \circ \\ \circ \end{array}. \tag{2.62}$$

The right-hand side of (2.61) contains three different graphical operations. The first two are linear and involve one or two line amputations of the previous perturbative order. The third operation is nonlinear and mixes two different one-line amputations of lower orders.

An alternative way of formulating the above recursion relation may be based on the graphical rules

$$W^{(p)} = \begin{array}{c} \circ \\ p \end{array}, \quad \frac{\delta W^{(p)}}{\delta G_{12}} = \begin{array}{c} 1 \\ \circ \\ 2 \end{array}, \quad \frac{\delta^2 W^{(p)}}{\delta G_{12} \delta G_{34}} = \begin{array}{c} 1 \\ 2 \\ \circ \\ 3 \\ 4 \end{array}. \tag{2.63}$$

With these, the recursion relation (2.61) reads

$$(p+1) \begin{array}{c} \circ \\ p \end{array} = 4 \begin{array}{c} \circ \\ p \end{array} + 12 \begin{array}{c} \circ \\ \circ \\ p \end{array} + 4 \sum_{q=1}^{p-1} \binom{p}{q} \begin{array}{c} \circ \\ p-q \end{array} \begin{array}{c} \circ \\ q \end{array}, \quad p \geq 1. \tag{2.64}$$

To demonstrate the working of (2.61), we calculate the connected vacuum diagrams up to five loops. Applying the linear operations to (2.60), we obtain immediately

$$\frac{\delta W^{(1)}}{\delta 1 \text{---} 2} = 6 \begin{array}{c} 1 \\ \circ \\ 2 \end{array}, \quad \frac{\delta^2 W^{(1)}}{\delta 1 \text{---} 2 \delta 3 \text{---} 4} = 6 \begin{array}{c} 1 \\ 2 \\ \circ \\ 3 \\ 4 \end{array}. \tag{2.65}$$

Inserted into (2.61), these lead to the three-loop vacuum diagrams

$$W^{(2)} = 24 \begin{array}{c} \circ \\ \circ \\ \circ \end{array} + 72 \begin{array}{c} \circ \\ \circ \\ \circ \end{array}. \tag{2.66}$$

Proceeding to the next order, we have to perform one- and two-line amputations on the vacuum graphs in (2.66), leading to

$$\frac{\delta W^{(2)}}{\delta 1 \text{---} 2} = 96 \begin{array}{c} 1 \\ \circ \\ 2 \end{array} + 144 \begin{array}{c} \circ \\ \circ \\ 1 \\ 2 \end{array} + 144 \begin{array}{c} \circ \\ \circ \\ 1 \\ 2 \end{array}, \tag{2.67}$$

and subsequently to

$$\begin{aligned}
\frac{\delta^2 W^{(2)}}{\delta 1-2 \delta 3-4} = & 288 \begin{array}{c} 1 \\ \diagdown \\ \circlearrowleft \\ \diagup \\ 2 \\ 3 \quad 4 \end{array} + 144 \begin{array}{c} 1 \\ \diagdown \\ \circlearrowleft \\ \diagup \\ 3 \\ 2 \quad 4 \end{array} + 288 \begin{array}{c} 1 \\ \circlearrowleft \\ 2 \\ \mid \\ 3 \\ \mid \\ 4 \end{array} \\
& + 144 \begin{array}{c} 1 \\ \circlearrowleft \\ 3 \\ \mid \\ 4 \\ \mid \\ 2 \end{array} + 144 \begin{array}{c} 2 \\ \circlearrowleft \\ 1 \\ \mid \\ 3 \\ \mid \\ 4 \end{array} + 144 \begin{array}{c} \circlearrowleft \\ 1 \\ \mid \\ 2 \\ \circlearrowleft \\ 3 \\ \mid \\ 4 \end{array} . \quad (2.68)
\end{aligned}$$

Inserting (2.67) and (2.68) into (2.61) and taking into account (2.65), we find the connected vacuum diagrams of order  $p = 3$  with their multiplicities as shown in Table I. We observe that the nonlinear operation in (2.61) does not lead to topologically new diagrams. It only corrects the multiplicities of the diagrams generated from the first two operations. This is true also in higher orders. The connected vacuum diagrams of the subsequent order  $p = 4$  and their multiplicities are listed in Table I.

As a cross-check we can also determine the total multiplicities  $M^{(p)}$  of all connected vacuum diagrams contributing to  $W^{(p)}$ . To this end we recall that each of the  $M^{(p)}$  diagrams in  $W^{(p)}$  consists of  $2p$  lines. The amputation of one or two lines therefore leads to  $2pM^{(p)}$  and  $2p(2p-1)M^{(p)}$  diagrams with  $2p-1$  and  $2p-2$  lines, respectively. Considering only the total multiplicities, the graphical recursion relations (2.61) reduce to the form derived before in Ref. [7]

$$M^{(p+1)} = 16p(p+1)M^{(p)} + 16 \sum_{q=1}^{p-1} \frac{p!}{(p-q-1)!(q-1)!} M^{(q)} M^{(p-q)}; \quad p \geq 1. \quad (2.69)$$

These are solved starting with the initial value

$$M^{(1)} = 3, \quad (2.70)$$

leading to the total multiplicities

$$M^{(2)} = 96, \quad M^{(3)} = 9504, \quad M^{(4)} = 1880064, \quad (2.71)$$

which agree with the results listed in Table I. In addition we note that the next orders would contain

$$M^{(5)} = 616108032, \quad M^{(6)} = 301093355520, \quad M^{(7)} = 205062331760640 \quad (2.72)$$

connected vacuum diagrams.

### III. SCALAR $\phi^2 A$ -THEORY

For the sake of generality, let us also study the situation where the quartic interaction of the  $\phi^4$ -theory is generated by a scalar field  $A$  from a cubic  $\phi^2 A$ -interaction. The associated energy functional

$$E[\phi, A] = E^{(0)}[\phi, A] + E^{(\text{int})}[\phi, A] \quad (3.1)$$

decomposes into the free part

$$E^{(0)}[\phi, A] = \frac{1}{2} \int_{12} G_{12}^{-1} \phi_1 \phi_2 + \frac{1}{2} \int_{12} H_{12}^{-1} A_1 A_2 \quad (3.2)$$

and the interaction

$$E^{(\text{int})}[\phi, A] = \frac{\sqrt{g}}{2} \int_{123} V_{123} \phi_1 \phi_2 A_3. \quad (3.3)$$

Indeed, as the field  $A$  appears only quadratically in (3.1), the functional integral for the partition function

$$Z = \int \mathcal{D}\phi \mathcal{D}A e^{-E[\phi, A]} \quad (3.4)$$

can be exactly evaluated with respect to the field  $A$ , yielding

$$Z = \int \mathcal{D} e^{-E^{(\text{eff})}[\phi]} \quad (3.5)$$

with the effective energy functional

$$E^{(\text{eff})}[\phi] = -\frac{1}{2} \text{Tr} \ln H^{-1} + \frac{1}{2} \int_{12} G_{12}^{-1} \phi_1 \phi_2 - \frac{g}{8} \int_{123456} V_{125} V_{346} H_{56} \phi_1 \phi_2 \phi_3 \phi_4. \quad (3.6)$$

Apart from a trivial shift due to the negative free energy of the field  $A$ , the effective energy functional (3.6) coincides with one (2.1) of a  $\phi^4$ -theory with the quartic interaction

$$V_{1234} = -3 \int_{56} V_{125} V_{346} H_{56}. \quad (3.7)$$

If we supplement the previous Feynman rules (2.7), (2.9) by the free correlation function of the field  $A$

$$1 \text{ --- } 2 \equiv H_{12} \quad (3.8)$$

and the cubic interaction

$$\text{---} \text{---} \text{---} \equiv \int_{123} V_{123}, \quad (3.9)$$

the intimate relation (3.7) between the  $\phi^4$ -theory and the  $\phi^2 A$ -theory can be graphically illustrated by

$$\text{---} \text{---} \text{---} = - \text{---} \text{---} \text{---} - \text{---} \text{---} \text{---} - \text{---} \text{---} \text{---}. \quad (3.10)$$

This corresponds to a photon exchange in the so-called  $s$ -,  $t$ - and  $u$ -channels of Mandelstam's theory of the scattering matrix. Their infinite repetitions yield the relevant forces in the Hartree, Fock and Bogoliubov approximations of many-body physics. In the following we analyze the  $\phi^2 A$ -theory along similar lines as before the  $\phi^4$ -theory.

### A. Perturbation Theory

Expanding the exponential in the partition function (3.4) in powers of the coupling constant  $g$ , the resulting perturbation series reads

$$Z = \sum_{p=0}^{\infty} \frac{1}{(2p)!} \left(\frac{g}{4}\right)^p \int \mathcal{D}\phi \mathcal{D}A \left( \int_{123456} V_{123} V_{456} \phi_1 \phi_2 \phi_4 \phi_5 A_3 A_6 \right)^p e^{-E^{(0)}[\phi, A]}. \quad (3.11)$$

Substituting the product of two fields  $\phi$  or  $A$  by a functional derivative with respect to the kernels  $G^{-1}$  or  $H^{-1}$ , we conclude from (3.11)

$$Z = \sum_{p=0}^{\infty} \frac{(-2g)^p}{(2p)!} \left( \int_{123456} V_{123} V_{456} \frac{\delta^3}{\delta G_{12}^{-1} \delta G_{45}^{-1} \delta H_{36}^{-1}} \right)^p e^{W^{(0)}}, \quad (3.12)$$

where the zeroth order of the negative free energy reads

$$W^{(0)} = -\frac{1}{2} \text{Tr} \ln G^{-1} - \frac{1}{2} \text{Tr} \ln H^{-1} \equiv \frac{1}{2} \text{---} \text{---} + \frac{1}{2} \text{---} \text{---}. \quad (3.13)$$

Inserting (3.13) in (3.12), the first-order contribution to the negative free energy yields

$$W^{(1)} = 2 \int_{123456} V_{123} V_{456} H_{36} G_{14} G_{25} + \int_{123456} V_{123} V_{456} H_{36} G_{12} G_{45}, \quad (3.14)$$

which corresponds to the Feynman diagrams

$$W^{(1)} = 2 \text{---} \text{---} + \text{---} \text{---} \text{---}. \quad (3.15)$$

## B. Functional Differential Equation for $W = \ln Z$

The derivation of a functional differential equation for the negative free energy  $W$  requires the combination of two independent steps. Consider first the identity

$$\int \mathcal{D}\phi \mathcal{D}A \frac{\delta}{\delta\phi_1} \left\{ \phi_2 e^{-E[\phi, A]} \right\} = 0, \quad (3.16)$$

which immediately yields with the energy functional (3.1)

$$\delta_{12}Z + 2 \int_3 G_{13}^{-1} \frac{\delta Z}{\delta G_{23}^{-1}} + 2\sqrt{g} \int_{34} V_{134} \frac{\delta \langle A_4 \rangle Z}{\delta G_{23}^{-1}} = 0, \quad (3.17)$$

where  $\langle A \rangle$  denotes the expectation value of the field  $A$ . In order to close the functional differential equation, we consider the second identity

$$\int \mathcal{D}\phi \mathcal{D}A \frac{\delta}{\delta A_1} e^{-E[\phi, A]} = 0, \quad (3.18)$$

which leads to

$$\langle A_1 \rangle Z = \sqrt{g} \int_{234} V_{234} H_{14} \frac{\delta Z}{\delta G_{23}^{-1}}. \quad (3.19)$$

Inserting (3.19) in (3.17), we result in the desired functional differential equation for the negative free energy  $W = \ln Z$ :

$$\delta_{12} + 2 \int_2 G_{13}^{-1} \frac{\delta W}{\delta G_{23}^{-1}} = -2g \int_{34567} V_{134} V_{567} H_{47} \left\{ \frac{\delta^2 W}{\delta G_{23}^{-1} \delta G_{56}^{-1}} + \frac{\delta W}{\delta G_{23}^{-1}} \frac{\delta W}{\delta G_{56}^{-1}} \right\}. \quad (3.20)$$

A subsequent separation (2.54) of the zeroth order (3.13) leads to a functional differential equation for the interaction part of the free energy  $W^{(\text{int})}$ :

$$\begin{aligned} \int_{12} G_{12}^{-1} \frac{\delta W^{(\text{int})}}{\delta G_{12}^{-1}} &= -\frac{g}{4} \int_{123456} V_{123} V_{456} H_{36} \{G_{12} G_{45} + 2G_{14} G_{25}\} + g \int_{123456} V_{123} V_{456} G_{12} H_{36} \frac{\delta W^{(\text{int})}}{\delta G_{45}^{-1}} \\ &\quad -g \int_{123456} V_{123} V_{456} H_{36} \left\{ \frac{\delta^2 W^{(\text{int})}}{\delta G_{12}^{-1} \delta G_{45}^{-1}} + \frac{\delta W^{(\text{int})}}{\delta G_{12}^{-1}} \frac{\delta W^{(\text{int})}}{\delta G_{45}^{-1}} \right\}. \end{aligned} \quad (3.21)$$

Taking into account the functional chain rules (2.56), (2.57), the functional derivatives with respect to  $G^{-1}$  in (3.21) can be rewritten in terms of  $G$ :

$$\begin{aligned} \int_{12} G_{12} \frac{\delta W^{(\text{int})}}{\delta G_{12}} &= \frac{g}{4} \int_{123456} V_{123} V_{456} H_{36} \{G_{12} G_{45} + 2G_{14} G_{25}\} + g \int_{123456} V_{123} V_{456} H_{36} \{G_{12} G_{47} G_{58} \\ &\quad + 2G_{14} G_{27} G_{58}\} \frac{\delta W^{(\text{int})}}{\delta G_{78}} + g \int_{123456789\bar{1}} V_{123} V_{456} H_{36} G_{17} G_{28} G_{39} G_{4\bar{1}} \left\{ \frac{\delta^2 W^{(\text{int})}}{\delta G_{78} \delta G_{9\bar{1}}} + \frac{\delta W^{(\text{int})}}{\delta G_{78}} \frac{\delta W^{(\text{int})}}{\delta G_{9\bar{1}}} \right\}. \end{aligned} \quad (3.22)$$

## C. Recursion Relation And Graphical Solution

The functional differential equation (3.22) is now solved by the power series

$$W^{(\text{int})} = \sum_{p=1}^{\infty} \frac{1}{(2p)!} \left(\frac{g}{4}\right)^p W^{(p)}. \quad (3.23)$$

Using the property (2.33) that the coefficients  $W^{(p)}$  satisfy the eigenvalue condition of the operator (2.32), we obtain both the recursion relation

$$\begin{aligned}
W^{(p+1)} &= 4(2p+1) \left\{ \int_{12345678} V_{123} V_{456} H_{36} (G_{12} G_{47} G_{58} + 2G_{14} G_{27} G_{58}) \frac{\delta W^{(p)}}{\delta G_{78}} \right. \\
&+ \left. \int_{123456789\bar{1}} V_{123} V_{456} H_{36} G_{17} G_{28} G_{39} G_{4\bar{1}} \left( \frac{\delta^2 W^{(p)}}{\delta G_{78} \delta G_{9\bar{1}}} + \sum_{q=1}^{p-1} \binom{2p}{2q} \frac{\delta W^{(p-q)}}{\delta G_{78}} \frac{\delta W^{(q)}}{\delta G_{9\bar{1}}} \right) \right\} \quad (3.24)
\end{aligned}$$

and the initial value (3.14). Using the Feynman rules (2.7), (3.8) and (3.9), the recursion relation (3.24) reads graphically

$$\begin{aligned}
W^{(p+1)} &= 4(2p+1) \left\{ \frac{\delta W^{(p)}}{\delta_{1 \rightarrow 2}} \begin{array}{c} 1 \\ \diagdown \\ \bullet \text{---} \text{---} \bullet \\ \diagup \\ 2 \end{array} \text{---} \text{---} \text{---} \bullet \quad + 2 \quad \frac{\delta W^{(p)}}{\delta_{1 \rightarrow 2}} \begin{array}{c} 1 \\ \text{---} \bullet \\ \text{---} \bullet \\ \text{---} \bullet \\ 2 \end{array} \right. \\
&+ \left. \frac{\delta^2 W^{(p)}}{\delta_{1 \rightarrow 2} \delta_{3 \rightarrow 4}} \begin{array}{c} 1 \\ \diagdown \\ \bullet \text{---} \text{---} \bullet \\ \diagup \\ 2 \\ \text{---} \bullet \\ \text{---} \bullet \\ 3 \\ \text{---} \bullet \\ \text{---} \bullet \\ 4 \end{array} \quad + \sum_{q=1}^{p-1} \binom{2p}{2q} \frac{\delta W^{(p-q)}}{\delta_{1 \rightarrow 2}} \begin{array}{c} 2 \\ \diagdown \\ \bullet \text{---} \text{---} \bullet \\ \diagup \\ 1 \end{array} \text{---} \text{---} \text{---} \begin{array}{c} 4 \\ \diagdown \\ \bullet \text{---} \text{---} \bullet \\ \diagup \\ 3 \end{array} \frac{\delta W^{(q)}}{\delta_{3 \rightarrow 4}} \right\}, \quad p \geq 1, \quad (3.25)
\end{aligned}$$

which is iterated starting from (3.15). In analogy to (2.64), this recursion relation can be cast in a closed diagrammatic way by using the alternative graphical rules (2.63):

$$\begin{aligned}
\textcircled{p+1} &= 4(2p+1) \left\{ \begin{array}{c} \textcircled{1} \text{---} \text{---} \bullet \text{---} \text{---} \textcircled{p} \\ \text{---} \bullet \text{---} \text{---} \textcircled{p} \end{array} \quad + 2 \quad \begin{array}{c} \textcircled{1} \text{---} \bullet \text{---} \bullet \text{---} \bullet \\ \text{---} \bullet \text{---} \bullet \text{---} \bullet \end{array} \textcircled{p} \\
&+ \begin{array}{c} \textcircled{1} \text{---} \bullet \text{---} \bullet \text{---} \bullet \\ \text{---} \bullet \text{---} \bullet \text{---} \bullet \end{array} \textcircled{p} \quad + \sum_{q=1}^{p-1} \binom{2p}{2q} \left( \textcircled{p-q} \text{---} \text{---} \bullet \text{---} \text{---} \textcircled{q} \right), \quad p \geq 1, \quad (3.26)
\end{aligned}$$

We illustrate the procedure of solving the recursion relation (3.25) by construction the three-loop vacuum diagrams. Applying one or two functional derivatives to (3.15), we have

$$\frac{\delta W^{(1)}}{\delta_{1 \rightarrow 2}} = 2 \begin{array}{c} 1 \\ \diagdown \\ \bullet \text{---} \text{---} \bullet \\ \diagup \\ 2 \end{array} \text{---} \text{---} \text{---} \bullet \quad + 4 \begin{array}{c} 1 \\ \text{---} \bullet \\ \text{---} \bullet \\ \text{---} \bullet \\ 2 \end{array}, \quad \frac{\delta^2 W^{(p)}}{\delta_{1 \rightarrow 2} \delta_{3 \rightarrow 4}} = 2 \begin{array}{c} 2 \\ \diagdown \\ \bullet \text{---} \text{---} \bullet \\ \diagup \\ 1 \end{array} \text{---} \text{---} \text{---} \begin{array}{c} 4 \\ \diagdown \\ \bullet \text{---} \text{---} \bullet \\ \diagup \\ 3 \end{array} \quad + 4 \begin{array}{c} 1 \\ \diagdown \\ \bullet \text{---} \text{---} \bullet \\ \diagup \\ 3 \end{array} \text{---} \text{---} \text{---} \begin{array}{c} 2 \\ \diagdown \\ \bullet \text{---} \text{---} \bullet \\ \diagup \\ 4 \end{array}. \quad (3.27)$$

This is inserted into (3.25) to yield the three-loop diagrams shown in Table IV with their multiplicities. The table also contains the subsequent 4-loop results which we shall not derive here in detail. Observe that the multiplicity of a connected vacuum diagram  $D$  in the  $\phi^2 A$ -theory is given by a formula similar to (2.10) in the  $\phi^4$ -theory:

$$M_{\phi^2 A}^D = \frac{(2p)! 4^p}{2!^{S+D} N}. \quad (3.28)$$

Here  $S$  and  $D$  denote the number of self- and double connections, whereas  $N$  represents the number of identical vertex permutations.

The connected vacuum diagrams of the  $\phi^2 A$ -theory in Table IV can, of course, be converted to corresponding ones of the  $\phi^4$ -theory in Table I, by shrinking wiggly lines to a point and dividing the resulting multiplicity by 3 in accordance with (3.10). This relation between connected vacuum diagrams in  $\phi^4$ - and  $\phi^2 A$ -theory is emphasized by the numbering used in Table IV. For instance, the shrinking converts the five diagrams #4.1-#4.5 in Table IV to the diagram #4 in Table I. Taking into account the different combinatorial factors in the expansion (2.6) and (3.23) as well as the factor 3 in the shrinkage (3.10), the multiplicity  $M_{\phi^4}^{E=0}$  of a  $\phi^4$ -diagram results from the corresponding one  $M_{\phi^2 A}^{E=0}$  of the  $\phi^2 A$ -partner diagrams via the rule

$$M_{\phi^4}^{E=0} = \frac{1}{(2p-1)!!} M_{\phi^2 A}^{E=0}. \quad (3.29)$$

#### IV. COMPUTER GENERATION OF DIAGRAMS

Continuing the solution of the graphical recursion relations (2.61) and (3.25) to higher loops becomes an arduous task. We therefore automatize the procedure by computer algebra. Here we restrict ourselves to the  $\phi^4$ -theory because of its relevance for critical phenomena.

##### A. Matrix Representation of Diagrams

To implement the procedure on a computer we must represent Feynman diagrams in the  $\phi^4$ -theory by algebraic symbols. For this we use matrices as defined in Refs. [8,9]. Let  $p$  be the number of vertices of a given diagram and label them by indices from 1 to  $p$ . Set up a matrix  $\mathbf{M}$  whose elements  $M_{ij}$  ( $0 \leq i, j \leq p$ ) specify the number of lines joining the vertices  $i$  and  $j$ . The diagonal elements  $M_{ii}$  ( $i > 0$ ) count the number of self-connections of the  $i$ th vertex. External lines of a diagram are labeled as if they were connected to a single additional dummy vertex with number 0. As matrix element  $M_{00}$  is set to zero as a convention. The off-diagonal elements lie in the interval  $0 \leq M_{ij} \leq 4$ , while the diagonal elements for  $i > 0$  are restricted by  $0 \leq M_{ii} \leq 2$ . We observe that the sum of the matrix elements  $M_{ij}$  in each row or column equals 4, where the diagonal elements count twice,

$$\sum_{j=0}^p M_{ij} + M_{ii} = \sum_{i=0}^p M_{ij} + M_{jj} = 4. \quad (4.1)$$

The matrix  $\mathbf{M}$  is symmetric and is thus specified by  $(p+1)(p+2)/2 - 1$  elements. Each matrix characterizes a unique diagram and determines its multiplicity via formula (2.28). From the matrix  $\mathbf{M}$  we read off directly the number of self-, double, triple, fourfold connections  $S, D, T, F$  and the number of external legs  $E = \sum_{i=1}^p M_{0i}$ . It also permits us to calculate the number  $N$  of identical vertex permutations. For this we observe that the matrix  $\mathbf{M}$  is not unique, since so far the vertex numbering is arbitrary. In fact,  $N$  is the number of permutations of vertices and external lines which leave the matrix  $\mathbf{M}$  unchanged [compare to the statement after (2.28)]. If  $n_M$  denotes the number of different matrices representing the same diagram, the number  $N$  is given by

$$N = \frac{p!}{n_M} \prod_{i=1}^p M_{0i}!. \quad (4.2)$$

The matrix elements  $M_{0i}$  count the number of external legs connected to the  $i$ th vertex. Inserting Eq. (4.2) into the formula (2.28) for  $E = 0$ , we obtain the multiplicity of the diagram represented by  $\mathbf{M}$ . This may be used to cross-check the multiplicities obtained before when solving the recursion relation (2.61).

As an example, consider the following diagram of the four-point function with  $p = 3$  vertices:



(4.3)

This diagram can be represented by altogether  $n_M = 3$  different matrices, depending on the labeling of the top vertex with two external legs by 1, 2, or 3:

$$\begin{array}{c}
 \begin{array}{c|cccc}
 & 0 & 1 & 2 & 3 \\
 \hline
 0 & 0 & 2 & 1 & 1 \\
 1 & 2 & 0 & 1 & 1 \\
 2 & 1 & 1 & 0 & 2 \\
 3 & 1 & 1 & 2 & 0
 \end{array}
 &
 \begin{array}{c|cccc}
 & 0 & 1 & 2 & 3 \\
 \hline
 0 & 0 & 1 & 2 & 1 \\
 1 & 1 & 0 & 1 & 2 \\
 2 & 2 & 1 & 0 & 1 \\
 3 & 1 & 2 & 1 & 0
 \end{array}
 &
 \begin{array}{c|cccc}
 & 0 & 1 & 2 & 3 \\
 \hline
 0 & 0 & 1 & 1 & 2 \\
 1 & 1 & 0 & 2 & 1 \\
 2 & 1 & 2 & 0 & 1 \\
 3 & 2 & 1 & 1 & 0
 \end{array}
 \end{array} . \quad (4.4)$$

From the zeroth row or column of these matrices or by inspecting the diagram (4.3), we read off that there exist two one-connections and one two-connection between external legs and vertices. Thus Eq. (4.2) states that the number of identical vertex permutations of the diagram (4.3) is 4 (compare the corresponding entry in Table III).

The matrix  $\mathbf{M}$  contains of course all information on the topological properties of a diagram [8,9]. For this we define the submatrix  $\tilde{\mathbf{M}}$  by removing the zeroth row and column from  $\mathbf{M}$ . This allows us to recognize the connectedness of

a diagram: A diagram is disconnected if there is a vertex numbering for which  $\tilde{\mathbf{M}}$  is a block matrix. Furthermore a vertex is a cutvertex, e.g. a vertex which links two otherwise disconnected parts of a diagram, if the matrix  $\tilde{\mathbf{M}}$  has an almost block-form for an appropriate numbering of vertices in which the blocks overlap only on some diagonal element  $\tilde{M}_{ii}$ , i.e. the matrix  $\tilde{\mathbf{M}}$  takes block form if the  $i$ th row and column are removed. Similarly, the matrix  $\tilde{\mathbf{M}}$  allows us to recognize a one-particle-reducible diagram, which falls into two pieces by cutting a certain line. Removing a line amounts to reducing the associated matrix elements in the submatrix  $\tilde{\mathbf{M}}$  by one unit. If the resulting matrix  $\tilde{\mathbf{M}}$  has block form, the diagram is one-particle-reducible.

So far, the vertex numbering has been arbitrary, making the matrix representation of a diagram non-unique. To achieve uniqueness, we proceed as follows. We associate with each matrix a number whose digits are composed of the matrix elements  $M_{ij}$  ( $0 \leq j \leq i \leq p$ ), i.e. we form the number with the  $(p+1)(p+2)/2 - 1$  elements

$$M_{10}M_{11}M_{20}M_{21}M_{22}M_{30}M_{31}M_{32}M_{33} \dots M_{pp}. \quad (4.5)$$

The smallest of these numbers is chosen to represent the diagram unique. For instance, the three matrices (4.4) carry the numbers

$$201101120, \quad 102101210, \quad 101202110, \quad (4.6)$$

the smallest one being the last. Thus we uniquely represent the diagram (4.3) by this number.

## B. Practical Generation

We are now prepared for the computer generation of Feynman diagrams. First the vacuum diagrams are generated from the recursion relation (2.61). From these the diagrams of the connected two- and four-point functions are obtained by cutting or removing lines. A MATHEMATICA program performs this task. The resulting unique matrix representations of the diagrams up to the order  $p = 4$  are listed in Table V–VII. They are the same as those derived before by hand in Table I–III. Higher-order results up to  $p = 6$ , containing all diagrams which are relevant for the five loop renormalization of the  $\phi^4$ -theory in  $d = 4 - \epsilon$  dimensions [9,18], are made available on internet [17], where also the program can be found.

### 1. Connected Vacuum Diagrams

The computer solution of the recursion relation (2.61) necessitates to keep an exact record of the labeling of external legs of intermediate diagrams which arise from differentiating a vacuum diagram with respect to a line once or twice. To this end we have to extend our previous matrix representation of diagrams where the external legs are labeled as if they were connected to a simple additional vertex with number 0. For each matrix representing a diagram we define an associated vector which contains the labels of the external legs connected to each vertex. This vector has the length of the dimension of the matrix and will be prepended to the matrix. By doing so, it is understood that the rows and columns of the matrix are labeled from 0 to the number of vertices as explained in Subsection IV.A, so that we may omit these labels from now on. Consider, as an example, the diagram (4.3) of the four-point function with  $p = 3$  vertices, where the spatial indices 1, 2, 3, 4 are assigned in a particular order:



$$. \quad (4.7)$$

In our extended matrix notation, such a diagram can be represented in total by six matrices:

$$\begin{pmatrix} \{\} & | & 0 & 2 & 1 & 1 \\ \{1,2\} & | & 2 & 0 & 1 & 1 \\ \{3\} & | & 1 & 1 & 0 & 2 \\ \{4\} & | & 1 & 1 & 2 & 0 \end{pmatrix}, \quad \begin{pmatrix} \{\} & | & 0 & 1 & 2 & 1 \\ \{3\} & | & 1 & 0 & 1 & 2 \\ \{1,2\} & | & 2 & 1 & 0 & 1 \\ \{4\} & | & 1 & 2 & 1 & 0 \end{pmatrix}, \quad \begin{pmatrix} \{\} & | & 0 & 1 & 1 & 2 \\ \{3\} & | & 1 & 0 & 2 & 1 \\ \{4\} & | & 1 & 2 & 0 & 1 \\ \{1,2\} & | & 2 & 1 & 1 & 0 \end{pmatrix}, \\ \begin{pmatrix} \{\} & | & 0 & 2 & 1 & 1 \\ \{1,2\} & | & 2 & 0 & 1 & 1 \\ \{4\} & | & 1 & 1 & 0 & 2 \\ \{3\} & | & 1 & 1 & 2 & 0 \end{pmatrix}, \quad \begin{pmatrix} \{\} & | & 0 & 1 & 2 & 1 \\ \{4\} & | & 1 & 0 & 1 & 2 \\ \{1,2\} & | & 2 & 1 & 0 & 1 \\ \{3\} & | & 1 & 2 & 1 & 0 \end{pmatrix}, \quad \begin{pmatrix} \{\} & | & 0 & 1 & 1 & 2 \\ \{4\} & | & 1 & 0 & 2 & 1 \\ \{3\} & | & 1 & 2 & 0 & 1 \\ \{1,2\} & | & 2 & 1 & 1 & 0 \end{pmatrix}. \quad (4.8)$$

In the calculation of the vacuum diagrams from the recursion relation (2.61), starting from the two-loop diagram (2.62), we have to represent three different elementary operations in our extended matrix notation:

1. Taking one or two derivatives of a vacuum diagram with respect to a line. For example, we apply this operation to the vacuum diagram #2 in Table I

$$\begin{aligned} \frac{\delta^2}{\delta G_{12} \delta G_{34}} \text{Diagram} &= 2 \frac{\delta}{\delta G_{12}} \left[ 3 \text{Diagram} + 4 \text{Diagram} \right] \\ &= 3 \left[ \text{Diagram} + \text{Diagram} + \text{Diagram} + \text{Diagram} \right]. \end{aligned} \quad (4.9)$$

This has the matrix representation

$$\begin{aligned} \frac{\delta^2}{\delta G_{12} \delta G_{34}} \begin{pmatrix} \{\} \\ \{\} \\ \{\} \end{pmatrix} \begin{pmatrix} 0 & 0 & 0 \\ 0 & 0 & 4 \\ 0 & 4 & 0 \end{pmatrix} &= 2 \frac{\delta}{\delta G_{12}} \left[ \begin{pmatrix} \{\} \\ \{3\} \\ \{4\} \end{pmatrix} \begin{pmatrix} 0 & 1 & 1 \\ 1 & 0 & 3 \\ 1 & 3 & 0 \end{pmatrix} + \begin{pmatrix} \{\} \\ \{4\} \\ \{3\} \end{pmatrix} \begin{pmatrix} 0 & 1 & 1 \\ 1 & 0 & 3 \\ 1 & 3 & 0 \end{pmatrix} \right] \\ &= 3 \left[ \begin{pmatrix} \{\} \\ \{1,3\} \\ \{2,4\} \end{pmatrix} \begin{pmatrix} 0 & 2 & 2 \\ 2 & 0 & 2 \\ 2 & 2 & 0 \end{pmatrix} + \begin{pmatrix} \{\} \\ \{2,3\} \\ \{1,4\} \end{pmatrix} \begin{pmatrix} 0 & 2 & 2 \\ 2 & 0 & 2 \\ 2 & 2 & 0 \end{pmatrix} + \begin{pmatrix} \{\} \\ \{1,4\} \\ \{2,3\} \end{pmatrix} \begin{pmatrix} 0 & 2 & 2 \\ 2 & 0 & 2 \\ 2 & 2 & 0 \end{pmatrix} + \begin{pmatrix} \{\} \\ \{2,4\} \\ \{1,3\} \end{pmatrix} \begin{pmatrix} 0 & 2 & 2 \\ 2 & 0 & 2 \\ 2 & 2 & 0 \end{pmatrix} \right]. \end{aligned} \quad (4.10)$$

The first and fourth matrix as well as the second and third matrix represent the same diagram in (4.9), as can be seen by permutating rows and columns of either matrix.

2. Combining two or three diagrams to one. We perform this operation by creating a block matrix of internal lines from the submatrices representing the internal lines of the original diagrams. Then the zeroth row or column is added to represent the respective original external spatial arguments. Let us illustrate the combination of two diagrams by the example

$$1 \text{Diagram} + 2 \text{Diagram} \equiv \begin{pmatrix} \{\} \\ \{1\} \\ \{2\} \end{pmatrix} \begin{pmatrix} 0 & 1 & 1 \\ 1 & 0 & 3 \\ 1 & 3 & 0 \end{pmatrix}, \quad \begin{pmatrix} \{\} \\ \{1,2\} \end{pmatrix} \begin{pmatrix} 0 & 2 \\ 2 & 1 \end{pmatrix} \rightarrow \begin{pmatrix} \{\} \\ \{1,2\} \\ \{1\} \\ \{2\} \end{pmatrix} \begin{pmatrix} 0 & 2 & 1 & 1 \\ 2 & 1 & 0 & 0 \\ 1 & 0 & 0 & 3 \\ 1 & 0 & 3 & 0 \end{pmatrix} \quad (4.11)$$

and the combination of three diagrams by

$$\begin{aligned} \text{Diagram} + \text{Diagram} + \text{Diagram} &\equiv \\ \begin{pmatrix} \{\} \\ \{1,2\} \end{pmatrix} \begin{pmatrix} 0 & 2 \\ 2 & 1 \end{pmatrix}, \quad \begin{pmatrix} \{\} \\ \{1,2,3,4\} \end{pmatrix} \begin{pmatrix} 0 & 4 \\ 4 & 0 \end{pmatrix}, \quad \begin{pmatrix} \{\} \\ \{3,4\} \end{pmatrix} \begin{pmatrix} 0 & 2 \\ 2 & 1 \end{pmatrix} &\rightarrow \begin{pmatrix} \{\} \\ \{1,2\} \\ \{1,2,3,4\} \\ \{3,4\} \end{pmatrix} \begin{pmatrix} 0 & 2 & 4 & 2 \\ 2 & 1 & 0 & 0 \\ 4 & 0 & 0 & 0 \\ 2 & 0 & 0 & 1 \end{pmatrix}. \end{aligned} \quad (4.12)$$

We observe that the ordering of the submatrices in the block matrix is arbitrary at this point, we just have to make sure to distribute the spatial labels of the external legs correctly.

3. Connecting external legs with the same label and creating an internal line. This is achieved in our extended matrix notation by eliminating the spatial labels of external legs which appear twice, and by performing an appropriate entry in the matrix for the additional line. Thus we obtain, for instance, from (4.11)

$$\text{Diagram} \equiv \begin{pmatrix} \{\} \\ \{\} \\ \{\} \\ \{\} \end{pmatrix} \begin{pmatrix} 0 & 0 & 0 & 0 \\ 0 & 1 & 1 & 1 \\ 0 & 1 & 0 & 3 \\ 0 & 1 & 3 & 0 \end{pmatrix} \quad (4.13)$$



and similarly from (4.12)

$$\text{Diagram} \equiv \left( \begin{array}{c|cccc} \{\} & 0 & 0 & 0 & 0 \\ \{\} & 0 & 1 & 2 & 0 \\ \{\} & 0 & 2 & 0 & 2 \\ \{\} & 0 & 0 & 2 & 1 \end{array} \right) . \quad (4.14)$$

As we reobtain at this stage connected vacuum diagrams where there are no more external legs to be labeled, we may omit the prepended vector.

The selection of a unique matrix representation for the resulting vacuum diagrams obtained at each stage of the recursion relation proceeds as explained in detail in Subsection IV.A. By comparing we find out which of the vacuum diagrams are topologically identical and sum up their individual multiplicities. Along these lines, the recursion relation (2.61) is solved by a MATHEMATICA program up to the order  $p = 6$ . The results are shown in Table V and in Ref. [17]. To each order  $p$ , the numbers  $n_p^{(0)}$  of topologically different connected vacuum diagrams are

$p$	1	2	3	4	5	6
$n_p^{(0)}$	1	2	4	10	28	97

(4.15)

## 2. Two- and Four-Point Functions $G_{12}$ and $G_{1234}^c$ from Cutting Lines

Having found all connected vacuum diagrams, we derive from these the diagrams of the connected two- and four-point functions by using the relations (2.18) and (2.25). In the matrix representation, cutting a line is essentially identical to removing a line as explained above, except that we now interpret the labels which represent the external spatial labels as sitting on the end of lines. Since we are not going to distinguish between trivially “crossed” graphs which are related by exchanging external labels in our computer implementation, we need no longer carry around external spatial labels. Thus we omit the additional vector prepended to the matrix representing a diagram when generating vacuum diagrams. As an example, consider cutting a line in diagram #3 in Table I

$$-\frac{\delta}{\delta G^{-1}} \text{Diagram} = 2 \text{Diagram} + \text{Diagram} + \text{Diagram} , \quad (4.16)$$

which has the matrix representation

$$-\frac{\delta}{\delta G^{-1}} \begin{pmatrix} 0 & 0 & 0 \\ 0 & 1 & 2 \\ 0 & 2 & 1 \end{pmatrix} = 2 \begin{pmatrix} 0 & 1 & 1 \\ 1 & 1 & 1 \\ 1 & 1 & 1 \end{pmatrix} + \begin{pmatrix} 0 & 2 & 0 \\ 2 & 0 & 2 \\ 0 & 2 & 1 \end{pmatrix} + \begin{pmatrix} 0 & 0 & 2 \\ 0 & 1 & 2 \\ 2 & 2 & 0 \end{pmatrix} . \quad (4.17)$$

Here the plus signs and multiplication by 2 have a set-theoretical meaning and are not to be understood as matrix algebra operations. The last two matrices represent, incidentally, the same graph in (4.16) as can be seen by exchanging the last two rows and columns of either matrix.

To create the connected four-point function, we also have to consider second derivatives of vacuum diagrams with respect to  $G^{-1}$ . If an external line is cut, an additional external line will be created which is not connected to any vertex. It can be interpreted as a self-connection of the zeroth vertex which collects the external lines. This may be accomodated in the matrix notation by letting the matrix element  $M_{00}$  count the number of lines not connected to any vertex. For example, taking the derivative of the first diagram in Eq. (4.16) gives

$$-\frac{\delta}{\delta G^{-1}} \text{Diagram} = \text{Diagram} + \text{Diagram} + \text{Diagram} + 2 \text{Diagram} , \quad (4.18)$$

with the matrix notation

$$-\frac{\delta}{\delta G^{-1}} \begin{pmatrix} 0 & 1 & 1 \\ 1 & 1 & 1 \\ 1 & 1 & 1 \end{pmatrix} = \begin{pmatrix} 0 & 3 & 1 \\ 3 & 0 & 1 \\ 1 & 1 & 1 \end{pmatrix} + \begin{pmatrix} 0 & 1 & 3 \\ 1 & 1 & 1 \\ 3 & 1 & 0 \end{pmatrix} + \begin{pmatrix} 0 & 2 & 2 \\ 2 & 1 & 0 \\ 2 & 0 & 1 \end{pmatrix} + 2 \begin{pmatrix} 1 & 1 & 1 \\ 1 & 1 & 1 \\ 1 & 1 & 1 \end{pmatrix}. \quad (4.19)$$

The first two matrices represent the same diagram as can be seen from Eq. (4.18). The last two matrices in Eq. (4.19) correspond to disconnected diagrams: the first because of the absence of a connection between the two vertices, the second because of the disconnected line represented by the entry  $M_{00} = 1$ . In the full expression for the two loop contribution  $G_{1234}^{c,(2)}$  to the four-point function in Eq. (2.25) all disconnected diagrams arising from cutting a line in  $G_{12}^{(2)}$  are canceled by diagrams resulting from the sum. Therefore we may omit the sum, take only the first term and discard all disconnected graphs it creates. This is particularly useful for treating low orders by hand. If we include the sum, we use the prescription of combining diagrams into one as described above in Subsection IV.B.1, except that we now omit the extra vector with the labels of spatial arguments.

### 3. Two- and Four-Point Function $\mathbf{G}_{12}$ and $\mathbf{G}_{1234}^c$ from Removing Lines

Instead of cutting lines of connected vacuum graphs once or twice, the perturbative coefficients of  $\mathbf{G}_{12}$  and  $\mathbf{G}_{1234}^c$  can also be obtained graphically by removing lines. Indeed, from (2.16), (2.44), (2.54) and (2.56) we get for the two-point function

$$\mathbf{G}_{12} = G_{12} + 2 \int_{34} G_{13} G_{24} \frac{\delta W^{(\text{int})}}{\delta G_{34}}, \quad (4.20)$$

so that we have for  $p > 0$

$$\mathbf{G}_{12}^{(p)} = 2 \int_{34} G_{13} G_{24} \frac{\delta W^{(p)}}{\delta G_{34}} \quad (4.21)$$

at our disposal to compute the coefficients  $\mathbf{G}_{12}^{(p)}$  from removing one line in the connected vacuum diagrams  $W^{(p)}$  in all possible ways. The corresponding matrix operations are identical to the ones for cutting a line so that in this respect there is no difference between both procedures to obtain  $\mathbf{G}_{12}$ .

Combining (4.20) with (2.12), (2.23) and (2.56), we get for the connected four-point function

$$\mathbf{G}_{1234}^c = 4 \int_{5678} G_{15} G_{26} G_{37} G_{48} \frac{\delta^2 W^{(\text{int})}}{\delta G_{56} \delta G_{78}} - 4 \int_{5678} G_{15} G_{27} (G_{36} G_{48} + G_{46} G_{38}) \frac{\delta W^{(\text{int})}}{\delta G_{56}} \frac{\delta W^{(\text{int})}}{\delta G_{78}} \quad (4.22)$$

which is equivalent to

$$\mathbf{G}_{1234}^{c,(p)} = 4 \int_{5678} G_{15} G_{26} G_{37} G_{48} \frac{\delta^2 W^{(p)}}{\delta G_{56} \delta G_{78}} - 4 \sum_{q=1}^{p-1} \binom{p}{q} \int_{5678} G_{15} G_{27} (G_{36} G_{48} + G_{46} G_{38}) \frac{\delta W^{(q)}}{\delta G_{56}} \frac{\delta W^{(p-q)}}{\delta G_{78}}. \quad (4.23)$$

Again, the sum serves only to subtract disconnected diagrams which are created by the first term, so we may choose to discard both in the first term.

Now the problem of generating diagrams is reduced to the generation of vacuum diagrams and subsequently taking functional derivatives with respect to  $G_{12}$ . An advantage of this approach is that external lines do not appear at intermediate steps. So when one uses the cancellation of disconnected terms as a cross check, there are less operations to be performed than with cutting. At the end one just interprets external labels as sitting on external lines. Since all necessary operations on matrices have already been introduced, we omit examples here and just note that we can again omit external labels if we are not distinguishing between trivially ‘‘crossed’’ graphs.

The generation of diagrams of the connected two- and four-point functions has been implemented in both possible ways. Cutting or removing one or two lines in the connected vacuum diagrams up to the order  $p = 6$  lead to the following numbers  $n_p^{(2)}$  and  $n_p^{(4)}$  of topologically different diagrams of  $\mathbf{G}_{12}^{(p)}$  and  $\mathbf{G}_{1234}^{c,(p)}$ :

$p$	1	2	3	4	5	6
$n_p^{(2)}$	1	3	8	30	118	548
$n_p^{(4)}$	1	2	8	37	181	1010

(4.24)

## V. OUTLOOK

In this work we have shown that all Feynman diagrams can be efficiently determined from a recursive graphical solution of a nonlinear functional differential equation order by order in the coupling strength. In separate publications, this method will be applied to the ordered phase of  $\phi^4$ -theory, where the energy functional contains a mixture of a cubic and a quartic interaction, and to quantum electrodynamics [19]. It is hoped that our method will eventually be combined with efficient numerical algorithms for actually evaluating these Feynman diagrams.

## ACKNOWLEDGEMENTS

We are thankful to Dr. Bruno van den Bossche and Florian Jasch for contributing various useful comments. One of us (M.B.) acknowledges support by the Studienstiftung des deutschen Volkes.

- 
- [1] J. Külbeck, M. Böhm, and A. Denner, *Comp. Phys. Comm.* **60**, 165 (1991).
  - [2] T. Hahn, hep-ph/9905354.
  - [3] <http://www-itp.physik.uni-karlsruhe.de/feynarts>.
  - [4] P. Nogueira, *J. Comput. Phys.* **105**, 279 (1993).
  - [5] <ftp://gtae2.ist.utl.pt/pub/qgraf>.
  - [6] H. Kleinert, *Fortschr. Phys.* **30**, 187 (1982).
  - [7] H. Kleinert, *Fortschr. Phys.* **30**, 351 (1982).
  - [8] J. Neu, MS Thesis (in German), FU-Berlin (1990).
  - [9] H. Kleinert, V. Schulte-Frohlinde, *Critical Properties of  $\phi^4$ -Theories*, World Scientific, in press.
  - [10] B. Kastening, *Phys. Rev.* **D 54**, 3965 (1996).
  - [11] B. Kastening, *Phys. Rev.* **D 57**, 3567 (1998).
  - [12] S.A. Larin, M. Mönnigmann, M. Strösser, V. Dohm, *Phys. Rev.* **B 58**, 3394 (1998).
  - [13] D.J. Amit, *Field Theory, the Renormalization Group and Critical Phenomena*, McGraw-Hill (1978).
  - [14] C. Itzykson, J.-B. Zuber, *Quantum Field Theory*, McGraw-Hill (1985).
  - [15] J. Zinn-Justin, *Quantum Field Theory and Critical Phenomena*, Third Edition, Oxford (1996).
  - [16] H. Kleinert, *Gauge Fields in Condensed Matter, Vol. I, Superflow and Vortex Lines*, World Scientific (1989).
  - [17] <http://www.physik.fu-berlin.de/~kleinert/294/programs>.
  - [18] H. Kleinert, J. Neu, V. Schulte-Frohlinde, K.G. Chetyrkin, S.A. Larin, *Phys. Lett.* **B 272**, 39 (1991); **319**, 545 (E) (1993).
  - [19] M. Bachmann, H. Kleinert, A. Pelster, hep-th/9907044.

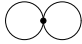
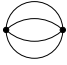
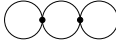

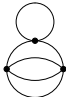
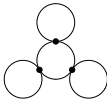

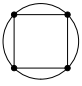
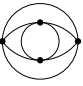
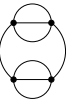
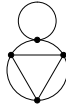
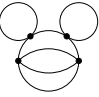
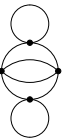
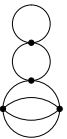
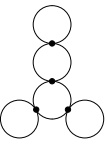
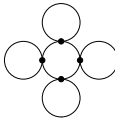

$p$	$W^{(p)}$							
1	<div style="display: flex; justify-content: center; align-items: center;"> <div style="text-align: center;"> <p>#1 3 (2,1,0,0;1)</p>  </div> </div>							
2	<div style="display: flex; justify-content: space-around; align-items: center;"> <div style="text-align: center;"> <p>#2 24 (0,0,0,1;2)</p>  </div> <div style="text-align: center;"> <p>#3 72 (2,1,0,0;2)</p>  </div> </div>							
3	<div style="display: flex; justify-content: space-around; align-items: center;"> <div style="text-align: center;"> <p>#4 1728 (0,3,0,0;6)</p>  </div> <div style="text-align: center;"> <p>#5 3456 (1,0,1,0;2)</p>  </div> <div style="text-align: center;"> <p>#6 1728 (3,0,0,0;6)</p>  </div> <div style="text-align: center;"> <p>#7 2592 (2,2,0,0;2)</p>  </div> </div>							
4	<div style="display: flex; justify-content: space-around; align-items: center;"> <div style="text-align: center;"> <p>#8 62208 (0,4,0,0;8)</p>  </div> <div style="text-align: center;"> <p>#9 248832 (0,2,0,0;8)</p>  </div> <div style="text-align: center;"> <p>#10 55296 (0,0,2,0;4)</p>  </div> <div style="text-align: center;"> <p>#11 497664 (1,2,0,0;2)</p>  </div> <div style="text-align: center;"> <p>#12 165888 (2,0,1,0;2)</p>  </div> </div> <div style="display: flex; justify-content: space-around; align-items: center;"> <div style="text-align: center;"> <p>#13 248832 (2,1,0,0;4)</p>  </div> <div style="text-align: center;"> <p>#14 165888 (1,1,1,0;2)</p>  </div> <div style="text-align: center;"> <p>#15 248832 (3,1,0,0;2)</p>  </div> <div style="text-align: center;"> <p>#16 62208 (4,0,0,0;8)</p>  </div> <div style="text-align: center;"> <p>#17 124416 (2,3,0,0;2)</p>  </div> </div>							

TABLE I. Connected vacuum diagrams and their multiplicities of the  $\phi^4$ -theory up to five loops. Each diagram is characterized by the vector  $(S, D, T, F; N)$  whose components specify the number of self-, double, triple and fourfold connections, and of the identical vertex permutations, respectively.



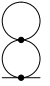

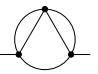
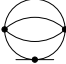
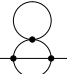
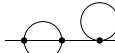
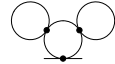


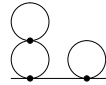
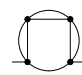
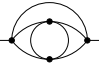
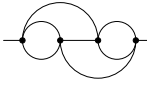
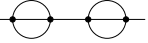
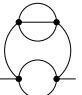

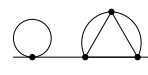
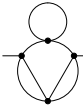
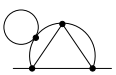
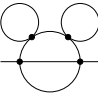
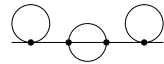
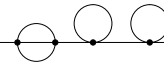
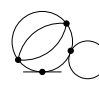
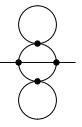
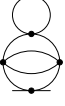
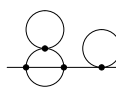
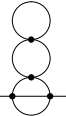
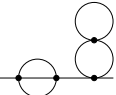
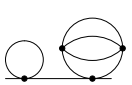
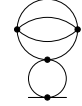
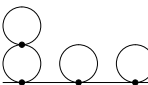
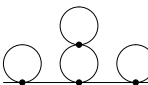
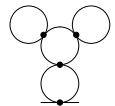
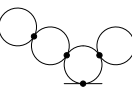
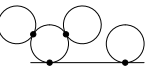
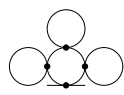
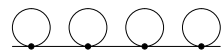
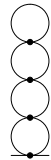
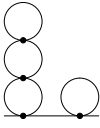
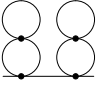

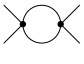
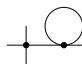
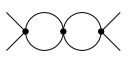
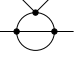
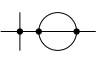
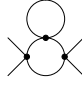
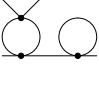
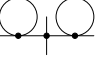
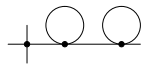
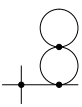
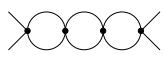
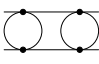
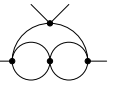
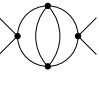
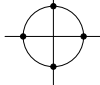
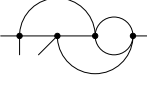
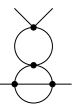
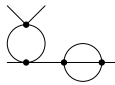
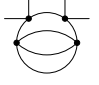
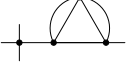
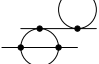
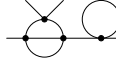
$p$	$G_{12}^{(p)}$						
1	#1.1 12  (1,0,0;2)						
2	#2.1 192  (0,0,1;2)	#3.1 288  (1,1,0;2)	#3.2 288  (2,0,0;2)				
3	#4.1 20736  (0,2,0;2)	#5.1 6912  (0,0,1;4)	#5.2 20736  (1,1,0;2)	#5.3 13824  (1,0,1;1)			
	#6.1 10368  (2,0,0;4)	#6.2 10368  (3,0,0;2)	#7.1 10368  (1,2,0;2)	#7.2 20736  (2,1,0;1)			
4	#8.1 995328  (0,3,0;2)	#9.1 1990656  (0,1,0;4)	#9.2 1990656  (0,2,0;2)	#10.1 221184  (0,0,2;2)	#10.2 663552  (0,1,1;2)		
	#11.1 995328  (0,2,0;4)	#11.2 1990656  (1,2,0;1)	#11.3 995328  (1,2,0;2)	#11.4 3981312  (1,1,0;1)	#12.1 995328  (2,1,0;2)		
	#12.2 331776  (2,0,1;2)	#12.3 663552  (2,0,1;1)	#12.4 663552  (1,0,1;2)	#13.1 995328  (2,0,0;4)	#13.2 995328  (1,1,0;4)		
	#13.3 1990656  (2,1,0;1)	#14.1 995328  (1,2,0;2)	#14.2 663552  (1,1,1;1)	#14.3 663552  (1,0,1;2)	#14.4 331776  (0,1,1;4)		
	#15.1 995328  (3,1,0;1)	#15.2 497664  (3,1,0;2)	#15.3 497664  (2,1,0;4)	#15.4 995328  (2,1,0;2)	#15.5 995328  (3,0,0;2)		
	#16.1 497664  (3,0,0;4)	#16.2 497664  (4,0,0;2)	#17.1 497664  (1,3,0;2)	#17.2 995328  (2,2,0;1)	#17.3 497664  (2,2,0;2)		

TABLE II. Connected diagrams of the two-point function and their multiplicities of the  $\phi^4$ -theory up to four loops. Each diagram is characterized by the vector  $(S, D, T; N)$  whose components specify the number of self-, double, triple connections, and of the identical vertex permutations, respectively.

$p$	$G_{1234}^{c,(p)}$
1	<p>#1.1.1 24 (0,0,0;24) </p>
2	<p>#2.1.1,#3.1.1 1152,576 1728 (0,1,0;8) </p> <p>#3.1.2,#3.2.1 1152,1152 2304 (1,0,0;6) </p>
3	<p>#4.1.1,#7.1.1 41472,20736 62208 (0,2,0;8) </p> <p>#4.1.2,#5.1.1,#5.2.1 165888,41472,41472 248832 (0,1,0;4) </p> <p>#5.1.2,#5.3.2 27648,27648 55296 (0,0,1;6) </p> <p>#5.2.2,#6.1.1 82944,41472 124416 (1,0,0;8) </p> <p>#5.2.3,#5.3.1,#7.1.2,#7.2.1 82944,82944,41472,41472 248832 (1,1,0;2) </p> <p>#6.1.2,#6.2.2,#7.2.2 20736,20736,82944 124416 (2,0,0;4) </p> <p>#6.1.3,#6.2.1 41472,41472 82944 (2,0,0;6) </p> <p>#7.1.3,#7.2.3 41472,41472 82944 (1,1,0;6) </p>
4	<p>#8.1.1,#17.1.1 1990656,995328 2985984 (0,3,0;8) </p> <p>#8.1.2,#9.2.1,#10.2.1 3981312,3981312,3981312 11943936 (0,2,0;4) </p> <p>#8.1.3,#11.1.2,#11.3.1 7962624,1990656,1990656 11943936 (0,2,0;4) </p> <p>#9.1.1,#13.2.1 3981312,1990656 5971968 (0,1,0;16) </p> <p>#9.1.2 7962624 (0,0,0;24) </p> <p>#9.1.3,#9.2.3,#11.1.1,#11.4.1 15925248,15925248,7962624,7962624 47775744 (0,1,0;2) </p> <p>#9.2.2,#14.1.1,#14.4.3 7962624,1990656,1990656 11943936 (0,2,0;4) </p> <p>#10.1.1,#10.2.3,#14.2.1,#14.4.2 2654208,2654208,1327104,1327104 7962624 (0,1,1;2) </p> <p>#10.2.2,#12.4.1 2654208,1327104 3981312 (0,0,1;8) </p> <p>#11.1.3,#11.2.1 3981312,3981312 7962624 (0,2,0;6) </p> <p>#11.2.2,#11.4.3,#14.1.2,#14.3.3 7962624,7962624,3981312,3981312 23887872 (1,1,0;2) </p> <p>#11.2.3,#11.4.2,#13.2.2,#13.3.1 7962624,7962624,3981312,3981312 23887872 (1,1,0;2) </p>

#11.2.4,#11.3.2,#17.1.2,#17.2.1 3981312,3981312,1990656,1990656 11943936 (1,2,0;2)		#11.3.3,#11.4.4,#12.1.1,#12.4.5 7962624,7962624,3981312,3981312 23887872 (1,1,0;2)		#11.4.5,#15.3.1,#15.4.1 7962624,1990656,1990656 11943936 (1,1,0;4)	
#11.4.6,#13.1.1,#13.2.3 15925248,3981312,3981312 23887872 (1,0,0;4)		#12.1.2,#12.2.2,#13.3.3,#17.2.2 1990656,1990656,3981312,3981312 11943936 (2,1,0;2)		#12.1.3,#16.1.2 3981312,1990656 5971968 (2,0,0;8)	
#12.1.4,#12.3.3,#15.1.1,#15.3.2 3981312,3981312,1990656,1990656 11943936 (2,1,0;2)		#12.2.1,#12.4.2 1327104,1327104 2654208 (1,0,1;6)		#12.3.2,#12.4.3,#14.2.2,#14.3.2 1327104,1327104,2654208,2654208 7962624 (1,0,1;2)	
#12.3.1,#12.4.4 1327104,1327104 2654208 (1,0,1;6)		#13.1.2,#13.3.4,#15.4.2,#15.5.1 7962624,7962624,3981312,3981312 23887872 (2,0,0;2)		#13.1.3,#16.1.1 1990656,995328 2985984 (2,0,0;16)	
#13.2.4,#13.3.5 3981312,3981312 7962624 (1,1,0;6)		#13.3.2,#15.2.1,#15.3.3 3981312,995328,995328 5971968 (2,1,0;4)		#14.1.3,#14.2.3,#17.1.3,#17.3.1 3981312,3981312,1990656,1990656 11943936 (1,2,0;2)	
#14.1.4,#15.4.4 3981312,1990656 5971968 (1,1,0;8)		#14.3.1,#14.4.1 1327104,1327104 2654208 (0,0,1;12)		#15.1.2,#15.5.3,#16.1.3,#16.2.2 3981312,3981312,1990656,1990656 11943936 (3,0,0;2)	
#15.1.3,#15.4.3,#17.2.3,#17.3.2 1990656,1990656,3981312,3981312 11943936 (2,1,0;2)		#15.1.4,#15.4.5 1990656,1990656 3981312 (2,1,0;6)		#15.2.2,#15.5.2 1990656,1990656 3981312 (3,0,0;6)	
#15.2.3,#15.4.6 1990656,1990656 3981312 (2,1,0;6)		#15.3.4,#15.5.4 1990656,1990656 3981312 (2,0,0;12)		#16.1.4,#16.2.1 1990656,1990656 3981312 (3,0,0;6)	
		#17.1.4,#17.2.4 1990656,1990656 3981312 (1,2,0;6)			

TABLE III. Connected diagrams of the four-point function and their multiplicities of the  $\phi^4$ -theory up to three loops. Each diagram is characterized by the vector  $(S, D, T; N)$  whose components specify the number of self-, double, triple connections, and of the identical vertex permutations, respectively.

$p$	$W^{(p)}$									
1	#1.1 2 (0,1;2)			#1.2 1 (2,0;2)						
2	#2.1 48 (0,0;8)		#2.2 24 (0,2;4)		#3.1 96 (0,0;4)		#3.2 96 (1,0;2)		#3.3 24 (2,1;2)	
3	#4.1 3840 (0,0;12)		#4.2 11520 (0,0;4)		#4.3 3840 (0,0;12)		#4.4 960 (0,3;6)		#4.5 5760 (0,1;4)	
	#5.1 11520 (0,1;2)		#5.2 23040 (0,0;2)		#5.3 11520 (1,0;2)		#5.4 5760 (1,1;2)		#6.1 7680 (0,0;6)	
	#6.2 11520 (1,0;2)		#6.3 5760 (2,0;2)		#6.4 960 (3,0;6)		#7.1 11520 (0,0;4)		#7.2 5760 (0,0;8)	
	#7.3 11520 (1,0;2)		#7.4 5760 (1,1;2)		#7.5 1440 (2,2;2)		#7.6 2880 (2,0;4)			

TABLE IV. Connected vacuum diagrams and their multiplicities of the  $\phi^2 A$ -theory up to four loops. Each diagram is characterized by the vector  $(S, D; N)$  whose components specify the number of self- and double connections as well as the identical vertex permutations, respectively.



$W^{(1)}$ : 1 diagram				
$i$	$j$			
1	1			
#	$M_{ij}$	$(S,D,T,F;N)$	$M$	$W^{-1}$
1	2	(2,1,0,0;1)	3	8

$W^{(2)}$ : 2 diagrams					
$i$	$j$				
1	22				
1	12				
#	$M_{ij}$	$(S,D,T,F;N)$	$M$	$W^{-1}$	
2	0	40	(0,0,0,1;2)	24	48
3	1	21	(2,1,0,0;2)	72	16

$W^{(3)}$ : 4 diagrams						
$i$	$j$					
1	22	333				
1	12	123				
#	$M_{ij}$	$(S,D,T,F;N)$	$M$	$W^{-1}$		
5	0	11	310	(1,0,1,0;2)	3456	24
4	0	20	220	(0,3,0,0;6)	1728	48
7	0	21	201	(2,2,0,0;2)	2592	32
6	1	11	111	(3,0,0,0;6)	1728	48

$W^{(4)}$ : 10 diagrams							
$i$	$j$						
1	22	333	4444				
1	12	123	1234				
#	$M_{ij}$	$(S,D,T,F;N)$	$M$	$W^{-1}$			
10	0	00	130	3100	(0,0,2,0;4)	55296	144
8	0	00	220	2200	(0,4,0,0;8)	62208	128
12	0	01	111	3100	(2,0,1,0;2)	165888	48
14	0	01	120	3010	(1,1,1,0;2)	165888	48
17	0	01	201	2200	(2,3,0,0;2)	124416	64
11	0	01	210	2110	(1,2,0,0;2)	497664	16
9	0	10	120	2110	(0,2,0,0;8)	248832	32
13	0	11	101	2110	(2,1,0,0;4)	248832	32
15	0	11	111	2001	(3,1,0,0;2)	248832	32
16	1	01	111	1101	(4,0,0,0;8)	62208	128

TABLE V. Unique matrix representation of all connected vacuum diagrams of  $\phi^4$ -theory up to the order  $p = 4$ . The number in the first column corresponds to their graphical representation in Table I. The matrix elements  $M_{ij}$  represent the numbers of lines connecting two vertices  $i$  and  $j$ , with omitting  $M_{i0} = 0$  for simplicity. The running numbers of the vertices are listed on top of each column in the first two rows. The further columns contain the vector  $(S, D, T, F; N)$  characterizing the topology of the diagram, the multiplicity  $M$  and the weight  $W = M/[(4!)^p p!]$ .

$G_{12}^{(1)}$ : 1 diagram					
$i$	11				
$j$	01				
#	$M_{ij}$	$(S,D,T;N)$	$M$	$W^{-1}$	
1.1	21	(1,0,0;2)	12	4	

$G_{12}^{(2)}$ : 3 diagrams					
$i$	11	222			
$j$	01	012			
#	$M_{ij}$	$(S,D,T;N)$	$M$	$W^{-1}$	
3.1	01	220	(1,1,0;2)	288	8
2.1	10	130	(0,0,1;2)	192	12
3.2	11	111	(2,0,0;2)	288	8

$G_{12}^{(3)}$ : 8 diagrams						
$i$	11	222	3333			
$j$	01	012	0123			
#	$M_{ij}$	$(S,D,T;N)$	$M$	$W^{-1}$		
7.1	00	021	2200	(1,2,0;2)	10368	16
5.1	00	030	2110	(0,0,1;4)	6912	24
5.3	00	111	1300	(1,0,1;1)	13824	12
4.1	00	120	1210	(0,2,0;2)	20736	8
6.1	01	011	2110	(2,0,0;4)	10368	16
7.2	01	101	1210	(2,1,0;1)	20736	8
5.2	01	110	1120	(1,1,0;2)	20736	8
6.2	01	111	1101	(3,0,0;2)	10368	16

$G_{12}^{(4)}$ : 30 diagrams							
$i$	11	222	3333	44444			
$j$	01	012	0123	01234			
#	$M_{ij}$	$(S,D,T;N)$	$M$	$W^{-1}$			
17.1	00	001	0220	22000	(1,3,0;2)	497664	32
12.4	00	001	0310	21100	(1,0,1;2)	663552	24
14.2	00	001	1120	13000	(1,1,1;1)	663552	24
11.3	00	001	1210	12100	(1,2,0;2)	995328	16
14.4	00	010	0130	22000	(0,1,1;4)	331776	48
11.1	00	010	0220	21100	(0,2,0;4)	995328	16
10.1	00	010	1030	13000	(0,0,2;2)	221184	72
9.2	00	010	1120	12100	(0,2,0;2)	1990656	8
15.3	00	011	0111	22000	(2,1,0;4)	497664	32
15.4	00	011	0201	21100	(2,1,0;2)	995328	16
13.2	00	011	0210	21010	(1,1,0;4)	995328	16
12.3	00	011	1011	13000	(2,0,1;1)	663552	24
13.3	00	011	1101	12100	(2,1,0;1)	1990656	8
11.4	00	011	1110	12010	(1,1,0;1)	3981312	4
11.2	00	020	1011	12100	(1,2,0;1)	1990656	8
8.1	00	020	1020	12010	(0,3,0;2)	995328	16
9.1	00	020	1110	11110	(0,1,0;4)	1990656	8
17.2	00	021	1001	12010	(2,2,0;1)	995328	16
14.1	00	021	1100	11020	(1,2,0;2)	995328	16
15.2	00	021	1101	11001	(3,1,0;2)	497664	32
14.3	00	030	1001	11110	(1,0,1;2)	663552	24
10.2	00	030	1010	11020	(0,1,1;2)	663552	24
12.2	00	030	1011	11001	(2,0,1;2)	331776	48
16.1	01	001	0111	21100	(3,0,0;4)	497664	32
15.1	01	001	1011	12100	(3,1,0;1)	995328	16
17.3	01	001	1020	12010	(2,2,0;2)	497664	32
13.1	01	001	1110	11110	(2,0,0;4)	995328	16
15.5	01	011	1001	11110	(3,0,0;2)	995328	16
12.1	01	011	1010	11020	(2,1,0;2)	995328	16
16.2	01	011	1011	11001	(4,0,0;2)	497664	32

TABLE VI. Unique matrix representation of all connected two-point function of  $\phi^4$ -theory up to the order  $p = 4$ . The numbers in the first column correspond to their graphical representation in Table II. The matrix elements  $M_{ij}$  represent the numbers of lines connecting two vertices  $i$  and  $j$ , with omitting  $M_{i0} = 0$  for simplicity. The running numbers of the vertices are listed on top of each column in the first two rows. The further columns contain the vector  $(S, D, T; N)$  characterizing the topology of the diagram, the multiplicity  $M$  and the weight  $W = M/[(4!)^p p!]$ .

$G_{1234}^{c,(1)}$ : 1 diagram				
$i$	11			
$j$	01			
#	$M_{ij}$	$(S,D,T;N)$	$M$	$W^{-1}$
1.1.1	40	(0,0,0;24)	24	24

$G_{1234}^{c,(2)}$ : 2 diagrams					
$i$	11	222			
$j$	01	012			
#	$M_{ij}$	$(S,D,T;N)$	$M$	$W^{-1}$	
3.1.2, 3.2.1	11	310	(1,0,0;6)	2304	12
2.1.1, 3.1.1	20	220	(0,1,0;8)	1728	16

$G_{1234}^{c,(3)}$ : 8 diagrams						
$i$	11	222	3333			
$j$	01	012	0123			
#	$M_{ij}$			$(S,D,T;N)$	$M$	$W^{-1}$
5.1.2, 5.3.2	00	130	3100	(0,0,1;6)	55296	36
4.1.1, 7.1.1	00	220	2200	(0,2,0;8)	62208	32
6.1.3, 6.2.1	01	111	3100	(2,0,0;6)	82944	24
7.1.3, 7.2.3	01	120	3010	(1,1,0;6)	82944	24
5.2.2, 6.1.1	01	210	2110	(1,0,0;8)	124416	16
5.2.3, 5.3.1, 7.1.2, 7.2.1	10	111	2200	(1,1,0;2)	248832	8
4.1.2, 5.1.1, 5.2.1	10	120	2110	(0,1,0;4)	248832	8
6.1.2, 6.2.2, 7.2.2	11	101	2110	(2,0,0;4)	124416	16

$G_{1234}^{c,(4)}$ : 37 diagrams							
$i$	11	222	3333	44444			
$j$	01	012	0123	01234			
#	$M_{ij}$				$(S,D,T;N)$	$M$	$W^{-1}$
13.2.4, 13.3.5	00	011	1210	31000	(1,1,0;6)	7962624	24
12.3.1, 12.4.4	00	011	1300	30100	(1,0,1;6)	2654208	72
11.4.5, 15.3.1, 15.4.1	00	011	2110	22000	(1,1,0;4)	11943936	16
11.1.3, 11.2.1	00	020	1120	31000	(0,2,0;6)	7962624	24
8.1.1, 17.1.1	00	020	2020	22000	(0,3,0;8)	2985984	64
9.1.1, 13.2.1	00	020	2110	21100	(0,1,0;16)	5971968	32
15.2.3, 15.4.6	00	021	1101	31000	(2,1,0;6)	3981312	48
17.1.4, 17.2.4	00	021	1200	30010	(1,2,0;6)	3981312	48
14.1.4, 15.4.4	00	021	2100	21010	(1,1,0;8)	5971968	32
12.2.1, 12.4.2	00	030	1011	31000	(1,0,1;6)	2654208	72
14.3.1, 14.4.1	00	030	1110	30010	(0,0,1;12)	2654208	72
10.2.2, 12.4.1	00	030	2010	21010	(0,0,1;8)	3981312	48
11.2.4, 11.3.2, 17.1.2, 17.2.1	00	101	1210	22000	(1,2,0;2)	11943936	16
12.3.2, 12.4.3, 14.2.2, 14.3.2	00	101	1300	21100	(1,0,1;2)	7962624	24
9.2.2, 14.1.1, 14.4.3	00	110	1120	22000	(0,2,0;4)	11943936	16
9.1.3, 9.2.3, 11.1.1, 11.4.1	00	110	1210	21100	(0,1,0;2)	47775744	4
10.1.1, 10.2.3, 14.2.1, 14.4.2	00	110	1300	20200	(0,1,1;2)	7962624	24
13.3.2, 15.2.1, 15.3.3	00	111	1101	22000	(2,1,0;4)	5971968	32
11.2.3, 11.4.2, 13.2.2, 13.3.1	00	111	1200	21010	(1,1,0;2)	23887872	8
8.1.3, 11.1.2, 11.3.1	00	120	1200	20110	(0,2,0;4)	11943936	16
15.1.4, 15.4.5	01	001	1120	31000	(2,1,0;6)	3981312	48
13.1.3, 16.1.1	01	001	2110	21100	(2,0,0;16)	2985984	64
16.1.4, 16.2.1	01	011	1011	31000	(3,0,0;6)	3981312	48
15.3.4, 15.5.4	01	011	1110	30010	(2,0,0;12)	3981312	48
12.1.3, 16.1.2	01	011	2010	21010	(2,0,0;8)	5971968	32
11.3.3, 11.4.4, 12.1.1, 12.4.5	01	100	1120	21100	(1,1,0;2)	23887872	8
14.1.3, 14.2.3, 17.1.3, 17.3.1	01	100	1210	20200	(1,2,0;2)	11943936	16
15.1.2, 15.5.3, 16.1.3, 16.2.2	01	101	1101	21100	(3,0,0;2)	11943936	16
13.1.2, 13.3.4, 15.4.2, 15.5.1	01	101	1110	21010	(2,0,0;2)	23887872	8
15.1.3, 15.4.3, 17.2.3, 17.3.2	01	101	1200	20110	(2,1,0;2)	11943936	16
12.1.4, 12.3.3, 15.1.1, 15.3.2	01	110	1101	20200	(2,1,0;2)	11943936	16
11.4.6, 13.1.1, 13.2.3	01	110	1110	20110	(1,0,0;4)	23887872	8
8.1.2, 9.2.1, 10.2.1	10	100	1120	12100	(0,2,0;4)	11943936	16
12.1.2, 12.2.2, 13.3.3, 17.2.2	10	101	1101	12100	(2,1,0;2)	11943936	16
11.2.2, 11.4.3, 14.1.2, 14.3.3	10	101	1110	12010	(1,1,0;2)	23887872	8
9.1.2	10	110	1110	11110	(0,0,0;24)	7962624	24
15.2.2, 15.5.2	10	111	1101	11001	(3,0,0;6)	3981312	48

TABLE VII. Unique matrix representation of all connected two-point function of  $\phi^4$ -theory up to the order  $p = 4$ . The numbers in the first column correspond to their graphical representation in Table III. The matrix elements  $M_{ij}$  represent the numbers of lines connecting two vertices  $i$  and  $j$ , with omitting  $M_{i0} = 0$  for simplicity. The running numbers of the vertices are listed on top of each column in the first two rows. The further columns contain the vector  $(S, D, T; N)$  characterizing the topology of the diagram, the multiplicity  $M$  and the weight  $W = M/[(4!)^p p!]$ .